Biogeosciences Discuss., 11, 2685–2733, 2014
www.biogeosciences-discuss.net/11/2685/2014/
doi:10.5194/bgd-11-2685-2014

Biogeosciences Discussions
Open Access

Coccolithophores on the north-west European shelf: calcification rates and environmental controls

A. J. Poulton[1], M. C. Stinchcombe[1], E. P. Achterberg[2,3], D. C. E. Bakker[4], C. Dumousseaud[2], H. E. Lawson[1,2], G. A. Lee[4], S. Richier[2], D. J. Suggett[5,6], and J. R. Young[7]

[1]National Oceanography Centre, University of Southampton Waterfront Campus, European Way, Southampton, UK
[2]Ocean and Earth Science, National Oceanography Centre Southampton, University of Southampton, Southampton, UK
[3]GEOMAR Helmholtz Centre for Ocean Research, 24148 Kiel, Germany
[4]Centre for Ocean and Atmospheric Sciences, School of Environmental Sciences, University of East Anglia, Norwich Research Park, Norwich, UK
[5]University of Essex, Essex, UK
[6]Plant Functional Biology and Climate Change Cluster, University of Sydney, Australia
[7]University College London, London, UK

Received: 21 January 2014 – Accepted: 24 January 2014 – Published: 18 February 2014

Correspondence to: A. J. Poulton (alex.poulton@noc.ac.uk)

Published by Copernicus Publications on behalf of the European Geosciences Union.

BGD
11, 2685–2733, 2014

Abstract

Coccolithophores are a key functional group in terms of the pelagic production of calcium carbonate (calcite), although their contribution to shelf-sea biogeochemistry, and how this relates to environmental conditions, is poorly constrained. Measurements of calcite production (CP) and coccolithophore abundance were made on the north-west European shelf to examine trends in coccolithophore calcification along natural gradients of carbonate chemistry, macronutrient availability and plankton composition. Similar measurements were also made in three bioassay experiments where nutrient (nitrate, phosphate) and pCO_2 levels were manipulated. Nanoflagellates (< 10 µm) dominated chlorophyll biomass and primary production (PP) at all but one sampling site, with CP ranging from 0.6–9.6 mmol C m^{-2} d^{-1}. Highest CP and coccolithophore cell abundance occurred in a diatom bloom in fully mixed waters off Helgoland, rather than in two distinct coccolithophore blooms in the central North Sea and Western English Channel. Estimates of coccolithophore contributions to total PP and nanoplankton PP were generally < 5 %, apart from in a coccolithophore bloom at the Western English Channel Observatory (E1) where coccolithophores contributed up to 11 % and at Helgoland where they contributed ~ 23 % to nanoplankton PP. Variability in CP was influenced by cell numbers, species composition and cell-normalised calcification rates under both in situ conditions and in the experimental bioassays. Water column structure and light availability had a strong influence on cellular calcification, whereas nitrate (N) to phosphate (P) ratios influenced bulk CP. Coccolithophore communities in the northern North Sea and over the Norwegian Trench showed responses to N and P addition whereas oceanic communities in the Bay of Biscay showed no response. Sharp decreases in pH and a rough halving of calcite saturation states in the bioassay experiments led to decreased CP in the Bay of Biscay and Northern North Sea, but not over the Norwegian Trench. These variable relationships to nutrient availability and changes in carbonate chemistry highlight the complex response of coccolithophore physiology to growth environment.

BGD
11, 2685–2733, 2014

1 Introduction

High cellular levels of calcite production in coccolithophores, maintained through the rapid production of individual cellular plates of calcite (coccoliths), facilitate this group with a strong influence on the marine carbon cycle through the production and export of calcite, as well as modification of air–sea carbon dioxide (CO_2) fluxes (Holligan et al., 1993a). As a group, coccolithophores are globally distributed, from the sub-polar Arctic to the Antarctic and from the open ocean to shelf seas. Coccolithophores have cell diameters of 5–10 µm, making them a potentially important component of the nanoflagellate (< 10 µm) community.

One of the most common coccolithophore species, *Emiliania huxleyi*, often forms large scale (50–250 × 10^3 km^2) blooms in the open ocean (e.g. Iceland Basin), along continental shelves (e.g. Patagonian Shelf) and in shelf seas (e.g. North Sea, English Channel) (Iglesias-Rodríguez et al., 2002; Tyrrell and Merico, 2004). Such blooms are characterised by the excessive production and shedding of coccoliths into the surrounding waters (Balch et al., 1996), giving a milky appearance and a high reflectance signature in satellite images (Holligan et al., 1983). Formation of *E. huxleyi* blooms is often linked to warm, stratified conditions where silicic acid concentrations are low (limiting diatoms), and irradiance levels are high (e.g. Holligan et al., 1983). Other factors, notably iron availability (Poulton et al., 2013), may also be important in further regulating bloom formation in cold, nutrient rich waters.

The north-west (NW) European Shelf was the first region where major coccolithophore blooms were recognised (Holligan et al., 1983, 1993b), and subsequent blooms in this area have been intensively studied (e.g. van der Wal et al., 1995; Head et al., 1998; Rees et al., 2002; Harlay et al., 2010, 2011). However, few studies have made observations during non-bloom conditions, in the context of the biomass and production of the phytoplankton community as a whole, and with reference to potentially growth-regulating environmental factors. Several factors are thought to be key in promoting oceanic bloom formation by coccolithophores, including shallow mixed lay-

BGD
11, 2685–2733, 2014

ers, high irradiances and temperatures, low nitrate to phosphate ratios, and reduced microzooplankton grazing (Iglesias-Rodríguez et al., 2002; Tyrrell and Merico, 2004).

Oceanic blooms may be > 250 000 km^2 in areal extent (Raitsos et al., 2006), with average rates of calcite production of ~ 1 g $CaCO_3$ m^{-2} d^{-1} (10 mmol C m^{-2} d^{-1}), standing stocks ~ 21 g $CaCO_3$ m^{-2} (210 mmol C m^{-2} d^{-1}) which scale to ~ 8.3×10^{12} g $CaCO_3$ for entire blooms (Holligan et al., 1993a). Blooms associated with continental shelves often tend to be smaller in areal extent (< 100 000 km^2) than oceanic features, with similar levels of calcite production (Harlay et al., 2010, 2011; Poulton et al., 2013) although species composition is a potentially important constraint on calcite standing stocks (Poulton et al., 2013). In contrast to oceanic regions where benthic calcite production is relatively low, benthic organisms in shallow shelf seas may exhibit significant calcite production and dominate shelf sea calcite production (Lebrato et al., 2010).

Shelf seas are also regions of extensive primary production, with 15 to 30 % of global primary production occurring in waters shallower than 200 m despite these areas constituting less than 10 % of the global ocean (Simpson and Sharples, 2012). Such high productivity is sustained by a seasonal shift in phytoplankton community composition from winter communities dominated by small (< 10 µm) flagellates to spring communities of highly productive diatoms (> 10 µm), and summer communities dominated again by small flagellates; however dinoflagellates and coccolithophores are also present during this time and may form sporadic but highly significant blooms (Widdicombe et al., 2010) in terms of shelf sea biogeochemistry.

The fraction of primary production associated with coccolithophore communities within this seasonal cycle is poorly constrained, with estimates only available for the open ocean and generally < 10 % (or up to 40 % during coccolithophore blooms; see Poulton et al., 2007, 2013). Such seasonality in phytoplankton community composition is driven by cycles in water-column stratification in spring through to summer and its breakdown in winter, and surface nutrient (nitrate, phosphate, silicate) drawdown during the stratified period; although strong tidal mixing can result in highly mixed areas throughout the year (Simpson and Sharples, 2012). During seasonal stratification,

BGD
11, 2685–2733, 2014

vertical segregation of the community also occurs, with picoplankton (< 0.2 µm) dominating upper nutrient impoverished waters and larger celled microplankton (> 10 µm; e.g. diatoms) occurring deeper in the nutrient enriched thermocline (Hickman et al., 2012).

The effect of global environmental change on marine organisms and ecosystems is a pressing concern in biological oceanography. Marine calcifiers, with their calcite (e.g. coccolithophores) and aragonite (e.g. pteropods) shells are of particular concern since they may be impacted by both global warming and ocean acidification: i.e. decreases in pH and mineral saturation states (e.g. calcite saturation state, Ω_C) as the oceans and seas take up anthropogenically released CO_2 (Royal Society, 2005). The broad aim of the present study was therefore to quantify coccolithophore production and how it varied in relation to key environmental drivers, such as nutrient availability and carbonate chemistry (pH, Ω_C), in waters around the NW European Shelf during summer (June) 2011 (Fig. 1).

Two approaches were used to examine coccolithophore dynamics: (1) in situ sampling at sites characterising different pelagic environments (e.g. stratified shelf, mixed shelf, oceanic) around the NW European Shelf; and (2) small-scale bioassay experiments where the natural communities were exposed to nutrient addition (nitrate, phosphate and silicate) and/or elevated pCO_2 (with a target of 750 µatm). In this paper we examine bulk community calcite production (CP), coccolithophore abundance and cellular levels of calcification (cell-normalised calcification or cell-CF) at the 14 sampling sites and within three of the bioassay experiments. A separate paper discusses coccolithophore morphological responses to pCO_2 in experimental manipulations and along environmental gradients (Young et al., 2014).

2 Methods

Sampling was carried out onboard the RRS *Discovery* (cruise number D366) which sailed from Liverpool (6 June 2011) to Liverpool (10 July 2011) around the NW Eu-

BGD
11, 2685–2733, 2014

ropean Shelf. Water sampling was carried out at 75 Conductivity-Temperature-Depth (CTD) stations, of which 14 pre-dawn (02:00 to 04:30 GMT) CTD stations (Fig. 1) were sampled at five light depths (55, 20, 14, 5 and 1 % of surface irradiance) for rate measurements (primary production, calcite production), biomass (chlorophyll *a*), phytoplankton community structure, macronutrients (nitrate+nitrate, phosphate, silicic acid) and carbonate chemistry.

The 14 sampling stations (Fig. 1, Table 1) were located at: Mingulay Reef (MRf), the Atlantic coast (Atl) off Ireland, the central Celtic Sea (Cel), the Western English Channel Observatory (E1), the Bay of Biscay (BB), the sampling site for the PEACE (Role of PElagic calcification And Export of CarbonatE production in climate change; Harlay et al., 2010, 2011) project (PEA), the southern North Sea (sNS), Helgoland Roads (Hel), the central North Sea (NS), south of the Shetland Islands (Sh) and south of the Faroe Islands (sFI). The Western English Channel Observatory (E1), Bay of Biscay (BB) and central North Sea (NS) were all sampled twice during the cruise either on consecutive days (BB, NS) or within 9 days (E1). The exact positions of these re-sampled locations were slightly different, especially in the case of BB and NS (Table 1).

Sea-surface temperatures and salinities were taken from the CTD, with mixed layer depths calculated using a temperature threshold difference of 0.5 °C relative to surface values (Painter et al., 2010) and visually checked by examining the temperature profiles (Fig. 2). Water-column structure was examined by calculating the Brunt-Väsälä frequency (N^2) from the density profile (Knauss, 1996):

$$N^2 = (g/\text{average}\sigma t)\cdot(\Delta\sigma t/\Delta z) \quad (1)$$

where g is acceleration due to gravity (9.81 m s^{-2}), average σt is the average density over the water-column at each site, $\Delta\sigma t$ is the difference in density between depth pairs and Δz is the difference in depth. N^2 estimates the strength of the vertical density gradient.

Daily incidental irradiance ($Ed_{[0+]}$), for Photosynthetically Active Radiation (PAR), was integrated from dawn to dusk (mol photons m^{-2} d^{-1}) from the RRS *Discovery* 2π

BGD
11, 2685–2733, 2014

PAR irradiance sensor (Skye Instruments, SKE 510). The vertical diffuse attenuation coefficient of PAR (K_d) in the water-column was calculated for pre-dawn CTD stations, with the depth of the euphotic zone (Z_{eup}) calculated as the depth where 1 % surface irradiance penetrates, with an optical depth of 4.6. Average mixed layer PAR irradiance ($\bar{E}d_{[ML]}$), which describes the mean irradiance experienced by a particle being mixed within the mixed layer, was calculated as in Poulton et al. (2011) using a combination of $Ed_{[0+]}$, K_d and mixed layer depth.

2.1 Coccolithophore counts and coccolith measurements

Samples for the determination of coccolithophore cell numbers and species identification by polarising light microscopy (see Young et al., 2014) were collected from the five light depths. Water samples (0.2–0.5 L) were filtered under gentle pressure through 25 mm diameter, 0.8 µm pore size Nuclepore™ cellulose nitrate filters, oven dried for ~ 2–4 h at 50–60 °C and stored in Petri-slides. Permanent slides of the filters were prepared immediately on-board by mounting the filters using low viscosity Norland Optical Adhesive (NOA 74) (Poulton et al., 2010). Coccolithophore cell counts and species identification were carried out under cross-polarised light using a Leitz Ortholux microscope (X1000, oil immersion). Either 300 fields of view or 300 individual cells (whichever reached first) were counted per filter, with a minimum of 30 fields of view counted when cells were abundant.

Measurements of detached *E. huxleyi* coccolith dimensions were made from Scanning Electron Microscopy (SEM) images following Poulton et al. (2011), with some minor modifications (see Young et al., 2014). Water samples (0.25–0.5 L), collected in parallel to those for light microscopy, were filtered through 25 mm diameter, 0.8 µm pore size Nuclepore™ polycarbonate filters under low vacuum, oven dried and stored in Petri-slides until SEM analysis. For SEM, a small portion of the filter was cut from the centre, mounted on an aluminium stub and coated in ~ 2 nm gold. A Leo 1450VP SEM (Carl Zeiss) with SmartSEM V5.1 software was then used to automatically capture images of consecutive fields of view (FOV) from a 10 × 11 FOV grid at a magnification of

BGD
11, 2685–2733, 2014

x5000, providing 110 images for analysis. These images were reviewed visually and all coccolithophores seen were collected as separate sub-images, using macro routines written in Image-J (http://rsbweb.nih.gov/ij/). In addition, the first 60 detached coccoliths seen in distal view were collected as separate sub-images. For each of these loose coccoliths, the coccolith length, width and thickness of the central tube were measured in Image-J (see Young et al., 2014). Coccolith lengths were converted to coccolith calcite content following Young and Ziveri (2000):

$$\text{Coccolith calcite(pmol C)} = 2.7 \times 0.02 \times \text{DSL}^3/100 \quad (2)$$

where 2.7 is the density of $CaCO_3$ ($g\,cm^3$), 0.02 is the shape constant for *E. huxleyi* (morphotype A), DSL is the distal shield length and 100 is the molecular weight of calcite.

2.2 Primary production and calcite production

Daily rates (dawn-dawn, 24 h) of total primary production and calcite production (CP) were determined at each of the 14 productivity stations following Poulton et al. (2010). Water samples (70 mL volume, 3 light, 1 formalin-killed) from the five light depths were spiked with 15–40 µCi of ^{14}C-labelled sodium bicarbonate, and placed in on-deck incubators chilled with surface sea-water and covered with light filters (Misty-blue and Grey, LEE™ UK) to replicate the light field at depth. Formalin-killed blanks were prepared by addition of 1 mL of 0.2 µm filtered and sodium borate-buffered formalin solution.

Incubations were ended by filtration through 25 mm 0.45 µm polycarbonate filters (Nuclepore™, US). Organic (PP) and inorganic (CP) carbon fixation was determined using the Micro-Diffusion Technique (MDT) (Paasche and Brutak, 1994; Balch et al., 2000) with filters placed in UltimaGold (Perkin-Elmer, UK) liquid scintillation cocktail and the activity on the filters determined using a TriCarb 2100TR Liquid Scintillation Counter. Spike activity was checked by removal of triplicate 100 µL sub-samples directly after spike addition, mixing with 200 µL of β-phenylethylamine (Sigma UK), addition of UltimaGold and liquid scintillation counting. Average relative standard deviation

BGD
11, 2685–2733, 2014

(RSD, standard deviation/mean ×100 %) of triplicate (light) total PP measurements was 14 % (2–47 %) and 38 % (2–93 %) for triplicate (light) CP measurements. On average the formalin-killed blank represented 10 % of the CP signal (range 1–63 %), with higher contributions at the base of the euphotic zone.

Daily rates (dawn-dawn, 24 h) of micro-phytoplankton (> 10 µm) primary production were determined in parallel to total PP. Water samples (70 mL volume, 3 light) were collected from the five light depths, spiked with 3–8 µCi of ^{14}C-labelled sodium bicarbonate and incubated on deck. Incubations were terminated by filtration through 25 mm 10 µm polycarbonate filters (Nuclepore^{TM}), with extensive rinsing with filtered seawater to remove any potential contamination from ^{14}C-labelled dissolved inorganic carbon. Finally, 15 mL UltimaGold (Perkin-Elmer, UK) liquid scintillation cocktail was added and the samples counted in the TriCarb Liquid Scintillation Counter. Spike activity was assessed as with total PP and the average RSD of triplicate microplankton PP measurements was 19 % (2–91 %). Nanoplankton PP (< 10 µm) was calculated as the difference between total PP and microplankton PP.

2.3 Chlorophyll *a*, macronutrients and carbonate chemistry

Total chlorophyll *a* (Chl) was quantified according to Poulton et al. (2010), with water samples (0.25 L) filtered onto Whatman GF/F filters, extracted in 8 mL 90 % acetone, and stored at 4 °C for 18–20 h. Fluorescence was measured on a Turner Designs Trilogy fluorometer, calibrated with purified chlorophyll *a* (Sigma, UK) and drift in the fluorometer was monitored using a solid standard. Chlorophyll in the > 10 µm fraction was measured on a 10 µm polycarbonate filter (0.25 L), with Chl in the < 10 µm fraction calculated as the difference between the two. Surface macronutrient (nitrate+nitrate, NO_x; phosphate, PO_4; silicic acid, dSi) concentrations were determined using an autoanalyser following standard protocols (Grasshoff et al., 1983).

The methodology for dissolved inorganic carbon (C_T) and total alkalinity (A_T) sampling and analysis from CTD samples followed Ribas-Ribas et al. (2014) and Bakker and Lee (2012), and is similar to Bakker et al. (2007). Duplicate water samples were

BGD
11, 2685–2733, 2014

drawn into 250 mL borosilicate glass bottles following Dickson et al. (2007). Samples were poisoned with 50 µL of a saturated mercuric chloride solution and analysed for C_T and A_T on a VINDTA 3C instrument (Marianda, Germany). Water samples were analyzed for C_T by the coulometric method after Johnson et al. (1987) with two to three CRMs (Certified Reference Material, batch 107) used for calibration per coulometric cell and station. Total alkalinity measurements were made by potentiometric titration with a Metrohm Titrino 719S for adding acid, an ORION-Ross pH electrode and a Metrohm reference electrode. The precision and accuracy for both A_T and C_T was $< 2\,\mu mol\,kg^{-1}$ for CTD samples.

Initial measurements for the short-term bioassays followed the sampling procedure of Dickson et al. (2007) with samples collected from CTD Niskin bottles in 250 mL Schott Duran borosilicate glass bottles with glass stoppers and analysed within one hour of collection. Samples from the end time point of the bioassays were collected in 40 mL glass vials, poisoned with a saturated solution of mercuric chloride and analysed within two days of collection. Dissolved inorganic carbon was determined using an Apollo AS-C3 (Apollo SciTech, USA) with a precision of 0.1 % or better. Phosphoric acid (10 %) was used to acidify the sample and the total amount of CO_2 released was quantified using a LI-COR (7000) CO_2 infrared analyser. Total alkalinity was determined using an Apollo AS-ALK2 (Apollo SciTech, USA) where each seawater sample was titrated with 0.1 M hydrochloric acid (Dickson et al., 2007). All A_T samples were analyzed at 25 °C (±0.1 °C) using a water bath (GD120, Grant, UK) to maintain temperature. The Apollo systems were calibrated daily using CRMs (batch 109). Calcite saturation state (Ω_C), pH_T and pCO_2 for both CTD samples and short-term bioassays were calculated from C_T, A_T, nutrients, temperature, salinity and pressure data using the CO2SYS (CO_2 system) program (v. 1.05; Pierrot et al., 2006) using the dissociation constants (pK's) of Mehrbach et al. (1973) as refit by Dickson and Millero (1987).

BGD
11, 2685–2733, 2014

2.4 Nutrient and pCO_2 bioassay

Near-surface seawater (< 10 m) was collected from three sites along the cruise track (Fig. 1) in order to conduct short-term (48 h) incubation experiments. These incubations are referred to as the "additional experiments" in Richier et al. (2014) rather than the longer (96 h) "main" experiments also performed during the June 2011 cruise. Table 4 indicates the oceanographic settings for each of the three additional bioassay experiments which were performed under precisely controlled light and temperature conditions in a purposely-converted commercial refrigeration container (see Methods in Richier et al., 2014). Briefly, 24 incubation bottles (1.25 L) were initially filled with unfiltered water containing the intact plankton communities. Seawater was supplemented with low levels of major macronutrients (nitrate, NO_x; phosphate, PO_4; dissolved silicic acid, dSi) according to an experimental design consisting of four conditions: (1) control, (2) 2 µmol kg^{-1} added NO_x and dSi, (3) 0.2 µmol kg^{-1} and 2 µmol kg^{-1} added PO_4 and dSi respectively, and (4) 2 µmol kg^{-1} added NO_x and dSi and 0.2 µmol kg^{-1} added PO_4 (hereafter control, +N, +P, +NP). A first set of triplicate bottles for each condition was kept at present day pCO_2, while a second set was adjusted to pCO_2 projected for the year 2100 (target 750 µatm CO_2, see Gattuso et al., 2010) (Table 4).

Carbonate chemistry manipulation in the incubation bottles followed the method described in Richier et al. (2014). Briefly, the initial carbonate chemistry in the seawater was characterized (see previous section) and subsequently manipulated in the incubation bottles using an equi-molar addition of strong acid (HCl, 1 mol kg^{-1}) and sodium bicarbonate ($NaHCO_3^-$, 1 mol kg^{-1}) (Gattuso et al., 2010). In addition, three independent bottles were measured at T_0 and checked for the accuracy of the method. After 48 h incubation, sub-samples were removed for determination of carbonate chemistry, macronutrient concentrations, chlorophyll *a* concentrations and coccolithophore cell abundances. Sub-samples were also removed and processed for determination of rates of primary production and calcite production. Methodology for all these measurements followed those detailed above for the in situ measurements.

BGD
11, 2685–2733, 2014

2.5 Statistical analysis

Pearson product-moment correlations (r) were performed in SigmaPlot (V11) to describe the correlations between coccolithophore dynamics and environmental variables. For treatment effects in the experimental bioassays one-way ANOVA (SigmaPlot V11.0) and pair-wise t tests were performed (SigmaPlot V11.0). For normally distributed data, one-way ANOVA and pair-wise Holm-Sidak comparisons were used, while for non-normally distributed data a Kruskal-Wallis one-way ANOVA on ranks and pair-wise Dunn comparison of the ranks was used.

3 Results

3.1 General hydrography

A number of distinct hydrographic environments were sampled around the NW European Shelf, including the open ocean (BB, PEA), shelf-break (MRf, Atl, Sh, sFl), seasonally stratified (Cel, E1, NS) and fully mixed (sNS, Hel) (Figs. 1 and 2). Open ocean sites generally had the deepest mixed layers (> 45 m), while mixed layer depths were similar for shelf-break and stratified sites (< 30 m) and fully mixed sites were mixed to the seafloor (~ 40 m) (Table 1, Fig. 2). There was a noticeable north-south gradient in mixed layer temperature of ~ 3–4 °C (Fig. 1a, Table 1), with sea-surface temperature at oceanic stations in the Bay of Biscay ~ 15 °C (Fig. 2).

Mixed layer salinities were generally > 34.8 except at the mixed sites (sNS, Hel), and off the Shetland Islands where values were 33.2 and 34.1 and as low as 30.7, respectively (Table 1). The maximum value of the Brunt-Väisälä Frequency (N^2) occurred south of the Shetland Islands ($3.53 \times 10^3\,m^{-1}$), but it was also high (0.4–$0.7 \times 10^3\,m^{-1}$) at stratified shelf sites including Cel, E1 and NS (Table 1). In contrast, the lowest values ($< 0.01 \times 10^3\,m^{-1}$) occurred at the fully mixed sites (sNS, Hel) and

BGD
11, 2685–2733, 2014

values < 0.3×10^3 m^{-1} were found at oceanic (BB, PEA) and shelf-break stations (MRf, Atl, sFI).

Euphotic zone depth (Z_{eup}) was generally > 24 m and showed little variability between hydrographic environments, although the shallowest euphotic zones (16–19 m) were at the fully mixed sites (sNS, Hel), likely due to sediment re-suspension. The ratio of mixed layer depth to euphotic zone depth was less than 1 at almost all sampling sites (see Table 1), apart from those associated with open-ocean conditions (BB, PEA) and at MRf, indicating that the potential for cells to be mixed into sub-euphotic zone irradiance conditions was limited to oceanic sites.

When expressed as the percentage of incident irradiance (i.e. $Ed_{[0+]}$), average mixed layer irradiance (an indication of the average irradiance experienced by cells in the mixed layer) was between 20–40 % for shelf-break and stratified sites, whereas it was < 20 % for oceanic sites (BB, PEA) and as low as 5–6 % for the fully mixed sites (sNS, Hel).

Daily photon fluxes for PAR ($Ed_{[0+]}$) varied during the cruise with values > 40 mol photons m^{-2} d^{-1} until the 24 June (E1b), increasing to > 60 mol photons m^{-2} d^{-1} during the next three days (sNS, Hel) before decreasing dramatically to < 24 mol photons m^{-2} d^{-1} for the remainder of the cruise (NS, Sh, sFI) as a result of bad weather in the North Sea. This temporal trend in incident irradiance translated into differences in absolute mixed layer irradiance values (Table 1) that were slightly different than the percentage values.

Average mixed layer irradiances at shelf-break sites varied from 9.4–14.6 mol photons m^{-2} d^{-1} (MRf, Atl) to 5.6–7.1 mol photons m^{-2} d^{-1} (Sh, sFI), and from 13.4–17.3 mol photons m^{-2} d^{-1} (Cel, E1) to 4.6–7.3 mol photons m^{-2} d^{-1} at stratified central North Sea sites. In the open-ocean, average mixed layer irradiance was 7.3–8.6 mol photons m^{-2} d^{-1} (BB, PEA), while low values were found at the fully mixed sites (3.0–3.3 mol photons m^{-2} d^{-1}) (Table 1).

Surface concentrations of NO_x, PO_4 and dSi at the stratified shelf sites (Cel, E1a, NS) were below 0.3 µmol kg^{-1}, 0.2 µmol kg^{-1} and 0.4 µmol kg^{-1}, respectively (Table 1,

BGD
11, 2685–2733, 2014

Fig. 2). The notable exception was on the second visit to E1 (E1b, 24 June) when surface concentrations of NO_x and dSi were elevated relative to initial conditions indicating a mixing event between visits. Sites near the shelf-break had higher NO_x (1.1–6.2 µmol kg^{-1}), PO_4 (0.1–0.4 µmol kg^{-1}) and dSi (0.6–2.1 µmol kg^{-1}) than stratified sites on the shelf, while open-ocean sites had NO_x ~ 0.3–1.1 µmol kg^{-1}, PO_4 < 0.1 µmol kg^{-1} and dSi 0.7–1.3 µmol kg^{-1} (Table 1, Fig. 2). The two mixed sites on the shelf had quite different nutrient concentrations, with Hel having higher NO_x (and dSi) values than sNS, while the two had similar PO_4 concentrations (Table 1, Fig. 2).

The value of N^*, expressed as $N^* = NO_x - 16 \cdot PO_4$ (e.g. Moore et al., 2009) was generally negative (MRf, E1, BB, PEA, sNS, NS, sFl) indicating low NO_x concentrations relative to PO_4, apart from at Atl, Hel and Sh which indicated high NO_x concentrations relative to low PO_4 (Table 1). Station Hel had the highest positive N^*, indicating high residual NO_x relative to PO_4, while station NSa had the lowest negative N^*. The value of Si^*, expressed as $Si^* = dSi - NO_x$ (e.g. Bibby and Moore, 2011), was negative at several sites (Atl, BBb, Hel, Sh, SFl), indicating low dSi concentrations relative NO_x, but positive at others (MRf, Cel, E1, BBa, PEA, sNs, NS) indicating enhanced dSi concentrations relative to low NO_x (Table 1). Stations MRf and PEA had the highest positive Si^* (1), indicating high residual dSi concentrations relative to nitrate, whereas stations sFl (−4.1) and Atl (−2.7) had the lowest negative Si^*.

Surface water pH_T values varied from 8.04 to 8.13, showing variability of less than 0.1 pH_T units between productivity stations, and was lowest in the sNS (Table 1). Calcite saturation states varied from 3.60 to 4.36, with the lowest value in the sNS, and the highest values at the open-ocean stations (BB, PEA) (Table 1).

3.2 In situ chlorophyll and primary production

Discrete measurements of total chlorophyll (Chl) varied from < 1 mg m^{-3} to a maximum of ~ 5 mg m^{-3} (Fig. 3). Vertical profiles of total Chl showed either uniform concentrations through the mixed layer and/or euphotic zone (e.g. Atl, E1, PEA) or deep maxima

BGD
11, 2685–2733, 2014

associated with the base of the mixed layer (e.g. Cel, Sh). Highest total Chl was found at the fully mixed Hel station and lowest Chl at the NS and BB sites (Fig. 3). Integrated euphotic zone total Chl concentrations ranged from 20.9 to 93.1 mg m^{-2} (Table 2), with generally low concentrations (< 30 mg m^{-2}) at the stratified shelf (Cel, E1, NS) and open ocean (BB) sites, although integrated total Chl was > 60 mg m^{-2} at the open ocean PEA site. Shelf-break sites had both moderate (40–45 mg m^{-2}, Atl, Sh, sFI) and high (> 90 mg m^{-2}) integrated total Chl, whereas mixed shelf sites had both low (< 30 mg m^{-2}, sNS) and high (> 80 mg m^{-2}, Hel) values (Table 2).

Integrated euphotic zone microplankton (> 10 µm) Chl varied from 2.6 to 78.0 mg m^{-2}, with highest values found at the mixed Hel site (data not shown). When expressed as a percentage of total Chl, nanoplankton Chl (< 10 µm) contributions ranged from 8 to 97 %, with the lowest value found at the Hel site (Table 2). At almost all sampling sites the < 10 µm fraction was the dominant contributor to total Chl, as shown in the scatter plot of total and microplankton integrated Chl (Fig. 4a). The exceptions were at the Hel site where microplankton Chl contributed 92 %, and at E1b where it was 55 % (Fig. 4a).

Discrete measurements of total primary production (PP) varied from < 0.1 to 6 mmol C m^{-3} d^{-1}, with low values generally at the base of the euphotic zone and highest rates at the Hel site (Fig. 3). In general, the vertical profiles of total PP (Fig. 3) showed high values in upper waters and decreased with depth (irradiance), with little or no evidence of sub-surface productivity maxima. Integrated euphotic zone total PP ranged from 45.2 to 229.9 mmol C m^{-2} d^{-1} (Table 2), with values between 45.2 to 128.6 mmol C m^{-2} d^{-1} in stratified shelf sites (Cel, E1, NS) and between 73.5 to 151.6 mmol C m^{-2} d^{-1} in shelf break sites (MRf, Atl, Sh, sFI). Open ocean sites (BB, PEA) had integrated total PP between 88.1 and 229.9 mmol C m^{-2} d^{-1} and the mixed shelf sites (sNS, Hel) had values between 89.5 and 197.9 mmol C m^{-2} d^{-1} (Table 2).

Integrated total Chl and total PP were significantly positively correlated (r = 0.76, $p < 0.005$, $n = 14$). Integrated microplankton (> 10 µm) PP varied from 3.8 to 169.3 mmol C m^{-2} d^{-1}, with the highest value at the Hel site (data not shown). When

BGD
11, 2685–2733, 2014

expressed as a percentage of total PP, nanoplankton PP ranged from 14 to 96 %, with the lowest contribution at the Hel site (Table 2). At almost all the productivity sites, the < 10 µm fraction was the dominant contributor to total PP (Table 2), as shown in the scatter plot of total and nanoplankton PP (Fig. 4b). The exception, again, was the Hel site where the microplankton fraction dominated PP (Fig. 4b).

3.3 In situ calcite production, coccolithophore abundance and cell-specific calcification

Discrete measurements of calcite production (CP) varied from < 10 to 825 µmol C m^{-3} d^{-1}, with low rates generally found at the base of the euphotic zone (Fig. 5). Vertical profiles of CP generally showed high rates near to the surface at the top of the euphotic zone and often these then decreased with increasing depth and were associated with decreasing irradiance, with no evidence of significant sub-surface peaks in CP (Fig. 5). Highest discrete measurements of CP were found in surface waters at Hel (> 700 µmol C m^{-3} d^{-1}) and lowest were found in the stratified shelf waters at Cel.

Integrated euphotic zone CP varied from 0.6 to 9.6 mmol C m^{-2} d^{-1}, with highest integrated CP at Hel (Table 2, Fig. 4c). Apart from the Atl and E1 sites, integrated CP was less than 3 mmol C m^{-2} d^{-1} for the other sampling sites. The ratio of integrated CP to PP varied from < 0.01 to 0.09, indicating that CP never contributed more than 10 % to the total carbon fixation (= CP + total PP). Highest CP to PP ratios were observed at E1a, whereas the site with the highest integrated CP (Hel) had a CP : PP ratio of only 0.05 (i.e. despite the highest discrete and integrated CP values at Hel, CP was only 5 % of total carbon fixation) (Table 2, Fig. 4c). CP showed no significant ($p > 0.1$) correlations with total Chl or PP, but did show significant ($p < 0.001$) relationships with microplankton Chl ($r = 0.80$, $n = 13$) and microplankton PP ($r = 0.79$, $n = 14$).

Discrete measurements of coccolithophore abundances ranged from < 1 cell mL^{-1} (Cel) to 898 cells mL^{-1} (Hel) across the 14 sampling sites (Fig. 5), and this abundance pattern agreed well with cell numbers averaged over the upper euphotic zone (< 30 m)

BGD
11, 2685–2733, 2014

(Table 3). Vertical profiles of coccolithophore cell numbers were slightly more variable with depth than CP profiles, although most profiles showed uniform or decreasing numbers with depth (Fig. 5). *Emiliania huxleyi* was the dominant species at most sites, typically representing more than 70 % of total cell numbers at all but a few sites (Cel, PEA) (Table 3). Other coccolithophore species present included *Gephyrocapsa muellerae*, *Syracosphaera* spp., *Coronosphaera mediterranea*, *Acanthoica quattrospina*, *Coccolithus pelagicus*, *Braarudosphaera bigelowii*, *Calcidiscus leptoporus*, and *Algirosphaera robusta* (Young et al., 2014). Offshore at the BB and PEA stations, *E. huxleyi* dominance was reduced (< 80 % total cells), with either *G. mullerae* (BB) or *Syracosphaera* spp. (PEA) becoming a significant component of the assemblage (Young et al., 2014).

Dividing CP by cell numbers allows calculation of cell specific rates (cell-CF), an index of cellular calcification by the species present (Poulton et al., 2010). Discrete measurements of cell-CF were generally $< 1.5\,\mathrm{pmol\,C\,cell^{-1}\,d^{-1}}$ apart from at Cel where they went up to over $30\,\mathrm{pmol\,C\,cell^{-1}\,d^{-1}}$ and deep in the water column at BB where they went up to $4\,\mathrm{pmol\,C\,cell^{-1}\,d^{-1}}$ (Fig. 6). In the case of Cel, LM cell counts were at the limit of detection ($\sim 1\,\mathrm{mL^{-1}}$) despite significant CP. Examination of surface SEM images from Cel observed $\sim 26\,\mathrm{cells\,mL^{-1}}$ (*A. quattrospina*, *Syracosphaera borealis* and an unidentified holococcolithophorid), which leads to a median recalculated cell-CF value of $1.5\,\mathrm{pmol\ C\ cell^{-1}d^{-1}}$ (Table 3). At the BB stations, *G. mullerae* represented 20–30 % of the total community in surface waters, and in the case of BBb it increased to equal numbers with *E. huxleyi* at depths where cell-CF was $> 3\,\mathrm{pmol\,C\,cell^{-1}\,d^{-1}}$ (Fig. 6). The vertical profiles of cell-CF generally showed either uniform or slight decreases with depth, with the notable exception of BBb where it increased below 22 m. Average cell-CF over the upper euphotic zone (< 30 m) (Table 3) generally agreed well with the vertical profiles (Fig. 5), ranging from 0.1 to $1.5\,\mathrm{pmol\ C\ cell^{-1}d^{-1}}$ at most sites.

Average distal shield lengths (DSL) for *E. huxleyi* ranged from 2.79 µm (BBb) to 3.49 µm (E1a) across the sampling sites (Table 3). Average DSL was < 3.2 µm at shelf break (MRf, Atl, Sh, sFl) and open-ocean (BB, PEA) stations and > 3.3 µm on the shelf stations, including both mixed (sNS, Hel) and most of the stratified (Cel, E1, NSa) sites

BGD
11, 2685–2733, 2014

apart from NSb (Table 3). Estimated coccolith calcite content, based on DSL, ranged from 0.012 pmol C (BB) to 0.023 pmol C (E1, sNS) (Table 3).

Dividing cell-CF by coccolith calcite content gives estimates of cellular levels of coccolith production (Poulton et al., 2010), which can be expressed per day or per hour (assuming, in this case, a 16 h day). Estimated coccolith production rates ranged from 0.4 h^{-1} to 8 h^{-1} (Table 3), with the exception of CeI which had excessively high cell-CF based on 1 cell mL^{-1} or a more "sensible" coccolith production rate of 4.4 h^{-1} when considering SEM based coccolithophore counts and a cell-CF of 1.5 pmol C $cell^{-1}$ (see above). For stations where *E. huxleyi* contributed > 99 % of total cells (Table 3), coccolith production rates ranged from 0.4 to 2.8 h^{-1}, with the highest rates occurring at the mixed sites (sNS, HeI). For stations where *E. huxleyi* represented < 80 % of total cells (Table 3), coccolith production rates ranged from 1.4 to 8.0 h^{-1}, with the highest rates generally occurring at the open ocean sites (BB, PEA) where *G. muellerae* and *Syracosphaera* spp. were important constituents of the community.

3.4 Co-variability of in situ data with environmental factors

Statistical comparisons (Pearson product moment correlations, r) were made between environmental factors (Table 1) and various coccolithophore metrics: CP, coccolithophore abundance, *E. huxleyi* relative abundance, cell-CF, coccolith calcite content and coccolith production rates. These comparisons were performed at three levels: (a) for all sampling stations, (b) only for stations where *E. huxleyi* was dominant (> 70 % of total cells) (Table 3), and (c) only for stratified stations (all apart from sNS and HeI). Due to the small dataset considered ($n < 15$), only correlations which were significant at $p < 0.01$ are presented here.

Integrated CP (Table 2) was positively correlated ($p < 0.01$) with N^* for all stations ($r = 0.72$, $n = 13$) and for the stratified sites ($r = 0.77$, $n = 10$), and strongly ($p < 0.001$) with mixed layer irradiance ($\bar{E}d_{[ML]}$) for sites where *E. huxleyi* dominated ($r = 0.91$, $n = 11$). Mixed layer average CP (Table 3) showed the same pattern, although with positive correlations with N^* for all stations ($r = 0.76$, $p < 0.005$, $n = 13$) and stratified

BGD
11, 2685–2733, 2014

sites ($r = 0.80$, $p < 0.01$, $n = 10$), and with $\bar{E}d_{[ML]}$ for sites where *E. huxleyi* dominated ($r = 0.90$, $p < 0.001$, $n = 11$).

Coccolithophore (total) cell abundances were negatively correlated with mixed layer depth (MLD) ($r = -0.75$, $p < 0.01$) and positively with $\bar{E}d_{[ML]}$ ($r = 0.72$, $p < 0.01$) for sites where *E. huxleyi* dominated ($n = 11$). *E. huxleyi* relative abundance was negatively correlated ($p < 0.001$) with MLD ($r = -0.89$) and the ratio of MLD to euphotic zone depth (Z_{eup}) ($r = -0.86$) at sites where *E. huxleyi* dominated ($n = 11$). *E. huxleyi* relative abundance was also negatively correlated ($p < 0.01$) to calcite saturation state (Ω_C) ($r = -0.66$) at all stations ($n = 13$). Cell-CF showed positive correlations with MLD at all sites ($r = 0.74$, $p < 0.005$, $n = 13$), at sites where *E. huxleyi* dominated ($r = 0.75$, $p < 0.01$, $n = 11$) and at stratified sites ($r = 0.91$, $p < 0.001$, $n = 10$). Cell-CF also showed positive correlations at stratified sites ($n = 10$) with the ratio of MLD to Z_{eup} ($r = 0.91$, $p < 0.001$) and incidental PAR ($Ed_{[0+]}$) ($r = 0.83$, $p < 0.005$). Coccolith calcite content showed correlations at all sites with Si^* ($r = 0.84$, $p < 0.005$, $n = 9$) and at stratified sites with mixed layer temperature ($r = 0.81$, $p < 0.01$, $n = 9$). Finally, rates of coccolith production were correlated with $Ed_{[0+]}$ at all sites ($r = 0.82$, $p < 0.01$, $n = 9$) and with MLD at stratified sites ($r = 0.95$, $p < 0.001$, $n = 9$).

3.5 Nutrient and pCO_2 bioassays

The results from the short-term (48 h) nutrient and pCO_2 bioassays are summarised in Fig. 7, which shows CP, coccolithophore cell abundances and cell-CF for the three experiments. Carbonate chemistry (pCO_2, pH_T, Ω_C), nutrient and total Chl concentrations in the bioassays are presented in Table 4. Additional variables (C_T, A_T, salinity, temperature and depth) are presented in Richier et al. (2014). pCO_2 treatments included an Ambient control and a targeted increase to ~ 750 µatm, whereas nutrient amendments included a control, a NO_x addition (+N), a PO_4 addition (+P) and a combined NO_x and PO_4 addition (+NP) (see Methods). Pair-wise *t* tests were used to test differences between ambient and 750 µatm treatments and one-way ANOVAs followed by pair-wise *t* tests were used to examine nutrient treatments effects (Fig. 7, see Methods).

BGD
11, 2685–2733, 2014

In the first bioassay (Bay of Biscay) initial and ambient pCO_2 levels were very similar (340 µatm and 330 to 341 µatm, respectively), as were pH_T values (~ 8.1) and Ω_C (4.4 and 4.3 to 4.5) (Table 4). Manipulation of pCO_2 levels led to a decrease in pH_T by 0.2–0.3 units between ambient and the 750 µatm target pCO_2 level at the end of the experiment and a rough halving of Ω_C to values ~ 2.6–2.7, while nutrient additions showed little drawdown over the 48 h of the extra 2 µM of NO_x or dSi, or 0.2 µM of PO_4 (Table 4). Total Chl was consistently higher by a factor of 2–3 between ambient and the high pCO_2 levels (Table 4). A similar decrease in nutrient drawdown and biomass in response to high pCO_2 was also observed after 48 h of incubation in a bioassay experiment (E3) set up at the same location (Richier et al., 2014). Significantly ($p < 0.05$) higher CP occurred in ambient treatments relative to the high pCO_2 treatment for all nutrient treatments apart from the +N treatment (Fig. 7a). A significant difference ($p < 0.05$) in cell numbers between ambient and high pCO_2 was only observed in the +NP treatment, while a significant ($p < 0.05$) difference in terms of cell-CF was only evident in the +P treatment (Fig. 7a). No significant differences were detected in one-way ANOVAs for the different nutrient treatments at either CO_2 level for CP ($p = 0.95$ for ambient, $p = 0.82$ for 750 µatm CO_2), cell numbers ($p = 0.95$ and $p = 0.09$, respectively) or cell-CF ($p = 0.25$ and $p = 0.41$, respectively).

For the second bioassay (Northern North Sea), carbonate chemistry differences between initial, ambient and the 750 µatm targeted pCO_2 level were very similar to the Bay of Biscay experiment: with a ~ 0.3 unit decrease in pH_T and a rough halving of Ω_C (2.2–2.3 vs. 4.0–4.1; Table 4). Nutrient additions again saw very little drawdown in terms of NO_x, PO_4 or dSi over the 48 h of the incubation, apart from in the ambient +NP treatment, where NO_x was reduced to 1.3 µM and PO_4 to 0.1 µM relative to the additions (Table 4). Total Chl concentrations were ~ 30–40 % higher in the ambient treatments relative to the initial and 750 µatm target pCO_2 treatments. Here again, nutrient consumption and biomass followed the same trend after a 48 h incubation period in the 96 h main bioassay set up in a similar area (Richier et al., 2014). In terms of CP, pair-wise t tests found significant ($p < 0.005$) differences between pCO_2 levels in

BGD
11, 2685–2733, 2014

both the +N and +NP treatments (Fig. 7b). No significant differences between pCO_2 treatments were observed in terms of cell numbers, however there were significant differences in cell-CF in the control treatments ($p < 0.05$) and +N treatment ($p < 0.005$). The second bioassay also showed a strong nutrient response under ambient conditions in CP, with significantly ($p < 0.05$) increased CP in the +NP treatments relative to the controls at ambient pCO_2 (Fig. 7b). No significant differences in terms of nutrient treatments were observed (one-way ANOVAs) at either pCO_2 level for either cell abundances ($p = 0.34$ for ambient, $p = 0.79$ for 750 µatm) or cell-CF ($p = 0.06$ and $p = 0.22$, respectively).

In the third bioassay (Norwegian Trench), carbonate chemistry differences between initial, ambient, and the 750 µatm targeted pCO_2 level were similar to the other experiments: with a ~ 0.3 unit decrease in pH_T and a rough halving of Ω_C (2.1 vs. 3.6–3.9; Table 4). Nutrient drawdown in the third experiment occurred in both the ambient and 750 µatm pCO_2 treatments, with similar decreases of NO_x and PO_4 independent of pCO_2 treatment in the +N and +P treatments. In contrast, in the +NP treatments, at both pCO_2 levels, there were larger decreases of NO_x (~ 0.8–1.0 µM) than in the single nutrient treatments (~ 0.4–0.6 µM). Total Chl was higher in +N and +NP treatments relative to the control and +P treatments, although the difference was lower in the 750 µatm target pCO_2 treatments than in the ambient (Table 4). In terms of CP, there was no significant difference with respect to pCO_2 level, but there was a significant (one-way ANOVA, $p < 0.05$) nutrient treatment effect with the +NP treatment being much higher than the control or +N at ambient pCO_2 (Fig. 7c). Cell numbers showed a significantly ($p < 0.05$) higher value between pCO_2 levels in the +NP treatment only, whereas cell-CF was significantly different ($p < 0.05$) between pCO_2 levels in the control treatment. Cell numbers also responded to nutrient amendment, with cell numbers being significant higher (one way ANOVA, $p < 0.05$) in the +NP treatment at ambient pCO_2 (Fig. 7c). Although there was a strong response to nutrients in the third bioassay, this was only found at ambient pCO_2, not at elevated pCO_2 and was completely absent in cell-CF at both pCO_2 levels ($p = 0.16$ for ambient and $p = 0.32$ for 750 µatm).

BGD
11, 2685–2733, 2014

4 Discussion

4.1 Coccolithophore production in NW European shelf waters

During June 2011, coccolithophores were a consistent component of phytoplankton communities around the NW European shelf, present at almost all sampling sites from open-ocean and shelf break communities to those in shelf waters under both stratified and mixed physical regimes. Following the spring diatom-dominated bloom, the phytoplankton community during summer 2011 was dominated by small (< 10 µm) autotrophs (Fig. 4, Table 2), apart from at a few sampling sites in specific environments such as Helgoland (Lawson, 2013). Estimates of coccolithophore contributions to total chlorophyll biomass and primary production were generally < 3 %, and < 5 % of nanoplankton (< 10 µm) primary production (Table 2). Exceptions to these low contributions were found during the first sampling of the coccolithophore bloom at the Western English Channel Observatory (E1) and in the diatom bloom (mainly *Guinardia flacccida*) at the Helgoland site (Lawson, 2013).

The high coccolithophore abundance (> 800 cells mL^{-1}) and high rates of CP at Helgoland (Fig. 5), alongside the highest total Chl and PP of the cruise (Table 2), are somewhat of a surprise. Although this site had the highest integrated CP of the entire cruise, rather than the coccolithophore blooms at E1 and North Sea sites, coccolithophores (*E. huxleyi*) still only contributed 3 % to total primary production, and ~ 20 % towards the small proportion of nanoplankton primary production occurring at this site (Table 2). A rough estimate of *E. huxleyi* Chl contribution, based on average mixed layer cell numbers (Table 3) and Chl (~ 4.5 mg m^{-3}) and a cellular Chl content of ~ 0.2 pg Chl $cell^{-1}$ (Haxo, 1985), indicates that *E. huxleyi* also only contributed ~ 4 % of total community Chl. Helgoland was also a fully mixed (bottom depth 42 m) site, with low mixed layer irradiances (< 3 mol photons m^{-2} d^{-1}), excess nitrate relative to phosphate, high dSi concentrations (Table 1) and large (> 50 µm) diatom cellular abundances > 60 cells mL^{-1} (Lawson, 2013); i.e. conditions not generally associated with

BGD
11, 2685–2733, 2014

intense coccolithophore blooms (see Iglesias-Rodríguez et al., 2002; Paasche, 2002; Tyrrell and Merico, 2004).

During June 2011, we also sampled several nanoflagellate dominated communities with integrated Chl > 60 mg m^{-2} and primary production > 150 mmol C m^{-2} d^{-1}, including Mingulay Reef and the PEACE site (Table 2). These nanoflagellate "blooms" were associated with shelf break and open ocean conditions, with coccolithophores (an obvious component of the nanoflagellate community) only representing ~ 1 % of nanoflagellate primary production (Table 3). In fact, despite the dominance of the nanoplankton size-range in shelf waters around the NW European shelf during summer, coccolithophores were not an important constituent of these communities.

Apart from Helgoland, we also sampled two other sites (E1, North Sea) with high (> 400 cells mL^{-1}) coccolithophore cell numbers and CP rates (Fig. 5) as well as high detached coccolith concentrations (> 40–50 × 10^{3} mL^{-1} based on SEM counts; Poulton, unpublished). In the case of E1, integrated CP was > 3 mmol C m^{-2} d^{-1}, while in the North Sea integrated CP was < 2 mmol C m^{-2} d^{-1} (Table 2). Other studies in shelf sea environments have observed a similar range of integrated CP values in bloom conditions: 1.2 to 11.5 mmol C m^{-2} d^{-1}, North Sea 1999 (Rees et al., 2002); 1.2 to 11.6 mmol C m^{-2} d^{-1}, Celtic Sea 2004 (Harlay et al., 2010); and 0.4–7.3 mmol C m^{-2} d^{-1}, Patagonian Shelf 2008 (Poulton et al., 2013). Satellite images have shown that the central North Sea bloom sampled during 2011 was at its most intense around 2–3 weeks before sampling (see Fig. 1 in Krueger-Hadfield et al., 2014), and hence our in situ measurements where post-bloom. At the E1 and North Sea sites, coccolithophore contributions to total and nanoplankton primary production (Table 2) were relatively low (< 10 % and < 25 %, respectively) compared with similar estimates in coccolithophore blooms (~ 30–40 %) (see Poulton et al., 2007, 2013).

Globally, coccolithophores are estimated to generally contribute 1–10 % of total primary production in open-ocean environments ranging from the subtropics to the subpolar Iceland Basin (Poulton et al., 2007, 2010). Hence, the low contributions in shelf waters around the NW European shelf (< 3 %) fit with the global picture of coccol-

BGD
11, 2685–2733, 2014

ithophores as minor contributors to total phytoplankton community biomass and primary production. Even within coccolithophore blooms, characterised by high concentrations of detached coccoliths and standing stocks of calcite, coccolithophores often represent < 40 % of total primary production (Poulton et al., 2007, 2013). Clearly, a major role of coccolithophores in pelagic communities is through the formation of calcite rather than primary production, and coccolithophores thus occupy the key role in global pelagic calcite production and export (Broecker and Clark, 2009).

4.2 Coccolithophore calcification in relation to hydrography and nutrients

Discrete measurements of CP generally decrease with irradiance through the water-column (Fig. 5), showing no obvious sub-surface maxima, even when sub-surface chlorophyll maxima were evident in the Chl profiles (e.g., Celtic Sea, E1b, Shetland; Fig. 3). The same lack of vertical structure is also seen in cell-CF (Fig. 6) and confirms earlier field observations of the strong (vertical) light-dependency of calcification (Poulton et al., 2007, 2010). Estimates of cell-CF also had a similar range (0.1–1.0 pmol C cell^{-1} d^{-1}; Table 3) to that found in other studies where *E. huxleyi* was dominant, for example the Iceland Basin (0.3–0.8 pmol C cell^{-1} d^{-1}; Poulton et al., 2010) and Patagonian Shelf (0.1–0.6 pmol C cell^{-1}d^{-1}; Poulton et al., 2013). Values above 1.5 pmol C cell^{-1}d^{-1} occurred at sites (Bay of Biscay, PEACE site) where other species (*G. muellerae*, *Syracosphaera* spp.) were present and which have potentially higher cellular inventories of calcite and hence higher cell specific rates, a trend also seen in Arctic cell-CF measurements where species other than *E. huxleyi* were present (Charalampopoulou et al., 2011).

In this study, cell-CF was correlated ($p < 0.01$) with mixed layer depth, with increasing cell-CF as mixed layers deepened at all sampling sites, as well at those where *E. huxleyi* dominated and at those that were stratified (Sect. 3.4). The highest cell-CF for *E. huxleyi* dominated communities in this study (0.8–1.0 pmol C cell^{-1} d^{-1}; Table 3) were found in the fully mixed sites in the Southern North Sea (sNS) and Helgoland. For stratified sites only, cell-CF was correlated ($p < 0.005$) with incidental PAR and the

BGD
11, 2685–2733, 2014

ratio of euphotic zone to mixed layer depth, whereas coccolith production rates were correlated ($p < 0.001$) with mixed layer depth. Clearly, water column structure and light availability had a strong influence on cellular calcification in waters around the NW European shelf, although no correlations where observed with mixed layer average irradiance. Instead, bulk community rates of CP (integrated and mixed layer averages) correlated ($p < 0.001$) with mixed layer average irradiance and coccolithophore cellular abundance ($p < 0.01$). Hence, mixed layer irradiance appeared to influence community size and CP, while water column structure had an influence on cellular calcification.

Absolute nutrient concentrations had little influence on bulk CP or cell-CF at the sampling sites in this study, whereas the nitrate to phosphate availability (expressed as N^*) was correlated ($p < 0.01$) with integrated and mixed layer average CP at all sites, as well as at those that were stratified. Interestingly, no correlations with N^* were found with CP at sites dominated by *E. huxleyi*, which highlights the more complex relationship between coccolithophore (*E. huxleyi*) activity and N : P ratios (Lessard et al., 2005) than originally proposed (Merico and Tyrrell, 2004). Coccolith calcite content for *E. huxleyi* was positively correlated with Si^* ($p < 0.005$) and mixed layer temperature ($p < 0.01$), indicating that calcite content per coccolith was high in warm mixed layers with low dSi concentrations relative to nitrate (i.e. Helgoland; see Tables 1 and 3).

The nutrient addition bioassays (Fig. 7) revealed variable responses from coccolithophores to the addition of nitrate (+N), phosphate (+P) or both (+NP), with the bioassays showing stronger coccolithophore responses to nutrient addition in shelf environments (Northern North Sea, Norwegian Trench) than in the open-ocean (Bay of Biscay). The response to nutrient addition was limited to the ambient pCO_2 treatments (see Sect. 4.3). In the Northern North Sea (Fig. 7b), community CP increased significantly ($p < 0.05$) in response to +NP addition, with the response being mediated by an increase in cell-CF, although no significant difference to the control was found. Around the Norwegian Trench (Fig. 7c), community CP also increased significantly ($p < 0.05$) in response to +NP addition and this response was mediated by a significant ($p < 0.05$) increase in cell numbers. In the open ocean (Fig. 7a), the coccolithophore community

BGD
11, 2685–2733, 2014

showed no response to nutrient addition, suggesting that other factors, such as light availability and/or micro-zooplankton grazing were regulating the coccolithophore community in the Bay of Biscay at the time of sampling.

Variability in community CP can be caused by changes in either the abundance of coccolithophore cells or cell-CF (Poulton et al., 2010), and it appears that both factors change in response to +NP during summer in shelf waters around the NW European Shelf (Fig. 7b, 7C). Estimating (net) growth rates based on the change in cell numbers between initial samples (dashed lines on Fig. 7) and samples 48 h later give rates ranging from 0.5–0.7 d^{-1} in the North Sea and 0.3–0.6 d^{-1} over the Norwegian Trench (data not shown). The sharp increase in CP over the Norwegian Trench is seen as an approximate doubling of net growth rates between the control (0.3 d^{-1}) and +NP (0.6 d^{-1}) treatments. In this bioassay, cell-CF was lower than initial values for all treatments apart from the +NP one which was approximately equal (0.6 pmol C $cell^{-1}$ d^{-1}) to the initial rate (0.7 pmol C $cell^{-1}$ d^{-1}) (Fig. 7c). In contrast, in the North Sea the net growth rates are similar across all treatments (0.6 d^{-1} in control and 0.7 d^{-1} in +NP), while the cell-CF in the +NP treatment (0.8 pmol C $cell^{-1}$ d^{-1}) is one of the few to be higher than the initial rate (0.5 pmol C $cell^{-1}$ d^{-1}).

Coccolithophores in shelf waters in summer 2011 only responded when both nitrate and phosphate were added together rather than one or the other alone, and responded through either an increased growth rate and stable cell-CF (Norwegian Trench, Fig. 7c) or through stable growth rates and increased cell-CF (North Sea, Fig. 7b). Nitrate and phosphate availability appeared to be the important factor regulating growth rates and cell-CF in NW European shelf waters (North Sea, Norwegian Trench) whereas other factors, such as irradiance and/or mortality, appeared more important in the open ocean (Bay of Biscay). This contrasts with the in situ results where cell-CF across the sampling sites only responded to descriptors of water-column structure and irradiance (mixed layer depth, incidental irradiance) and highlights how changes in bulk CP should be viewed with caution unless detailed information is available with which to examine

BGD
11, 2685–2733, 2014

whether variability in cell numbers and/or cell-CF is responsible (Poulton et al., 2010, 2013).

4.3 Coccolithophore calcification in relation to carbonate chemistry

In situ measurements showed only one relationship to a parameter of the carbonate chemistry: a significant ($p < 0.01$) inverse correlation between pH_T and *E. huxleyi* dominance. Across the sites sampled around the NW European shelf in June 2011, pH_T varied by ~ 0.09 units (8.04 to 8.13) while calcite saturation state (Ω_C) varied by ~ 0.7 units (3.60 to 4.36). Hence, this scale of variability in either pH_T or Ω_C appeared not enough to show a clear impact on the coccolithophore community in shelf waters in summer. In contrast, Charalampopoulou et al. (2011) found a change in species composition with variability in pH_T of 0.4 units (8.05 to 8.45) and 0.9 units (3.5 to 4.4) in Ω_C along a transect from the North Sea to the Arctic. Similarly, Smith et al. (2012) observed changes in dominant *E. huxleyi* morphotypes in the Bay of Biscay between winter and summer with changes in pH_T of ~ 0.06 units (8.06 to 8.13) and ~ 1.6 units (3.6 to 5.2) in Ω_C. However, Poulton et al. (2011, 2013) found differences of ~ 0.4 units (7.9 to 8.3) of pH_T and ~ 2.3 units (3.2 to 5.5) of Ω_C along the Patagonian Shelf, with the *E. huxleyi* bloom at that time in waters at the low end of both the pH and Ω_C gradient. Clearly, the response of coccolithophore CP and community composition to carbonate chemistry is more complex than a simple inverse linear response.

Importantly, around the NW European Shelf in June 2011 no co-variability of pH/Ω_C was observed with other growth-limiting factors (e.g. temperature). This contrasts with other studies where variability in coccolithophore dynamics across pH/Ω_C gradients (e.g. Charalampopoulou et al., 2011; Smith et al., 2012; Poulton et al., 2011, 2013) are associated with co-varying gradients in growth-limiting factors such as temperature, nutrient concentrations and light availability. This contrast in coccolithophore response to pH/Ω_C, between gradients where carbonate chemistry co-varies with other environmental parameters and gradients where there is no co-variability, is key to interpreting

BGD
11, 2685–2733, 2014

coccolithophore eco-physiology in relation to growth-limiting factors and needs to be carefully considered in future studies.

With this context in mind, it is useful to consider the pCO_2 and nutrient manipulation experiments carried out in June 2011. In this case, the pH_T and Ω_C conditions were changed drastically compared with the natural gradients present in June 2011, with pH_T reduced by ~ 0.3 units and Ω_C reduced by ~ 1.8 units (Table 4). Such changes were enforced on the ambient populations within < 12 h, which represents a much faster shift in carbonate chemistry than will be experienced through ocean acidification over the next century. Hence, the bioassays tested coccolithophore sensitivity to sharp changes in carbonate chemistry rather than acclimation to ocean acidification processes occurring over decades per se. In this context, even results generated through long-term experiments (Lohbeck et al., 2012; Jin et al., 2013) must be interpreted with caution, as the time scale is still an order of magnitude lower than the hundreds of generation/adaptation periods of microbes to ocean acidification in nature (Richier et al., 2014).

Given these abrupt changes in carbonate chemistry (pH_T, Ω_C), strong differences in CP, cell numbers and cell-CF between ambient and the higher pCO_2 treatment (750 µatm pCO_2 target) are not unsurprising (Fig. 7). An effect of increasing pCO_2 was observed in all three bioassays, although it was more evident in the first two (Bay of Biscay, North Sea) than the third (Norwegian Trench). As with the response to nutrient addition, the response to sharp changes in pH_T and Ω_C were seen in both cell numbers and cell-CF. In the Norwegian Trench bioassay (Fig. 7a), significant ($p < 0.05$) reductions in CP between ambient and elevated pCO_2 were linked to decreases in cell numbers (and growth rates: 0.1 d^{-1} in high pCO_2 and 0.5 d^{-1} in ambient) in the +NP treatment and decreases in cell-CF in the +P treatment. In the North Sea bioassay (Fig. 7b), significant ($p < 0.005$) reductions in CP were linked to decreases in cell-CF in the control and +N treatment, and in the case of +NP a sharp increase in cell-CF under ambient conditions (0.8 pmol C $cell^{-1}$ d^{-1}), while the cell-CF under elevated pCO_2 (0.4 pmol C $cell^{-1}$ d^{-1}) was more similar to the initial cell-CF (0.5 pmol C $cell^{-1}$ d^{-1}). In

BGD
11, 2685–2733, 2014

the third bioassay over the Norwegian Trench (Fig. 7c), no clear differences in CP were evident and (net) growth rates were relatively slow (0.2–0.4 d^{-1}) in all treatments apart from +NP (0.6 d^{-1}) under ambient conditions, and the coccolithophore community here seemed the least sensitive to extreme pCO_2 changes over 48 h.

Across the three experiments, CP was noticeably higher than initial values in only the ambient conditions, apart from in the third bioassay where only the +NP treatments were higher (Fig. 7). This trend is in contrast to that seen in cell numbers: cell numbers were higher in both ambient and elevated pCO_2 treatments relative to the initial values, apart from in the case of +NP in the first bioassay (Fig. 7a), and hence the coccolithophore communities almost always had positive (net) growth rates, despite the pCO_2 manipulation. For cell-CF, the first bioassay (Bay of Biscay) had similar values at the end relative to the initial, while in the second bioassay, and especially in the third, cell-CF was lower than initial values (Fig. 7). Again, the coccolithophore response to experimental manipulation (in this case via pCO_2) was mediated by changes in cell numbers (growth rates) and cell-CF, and the sensitivity of the different communities sampled to extreme pCO_2 changes was highly variable. This pattern of response (i.e., changes in growth rate and/or cell-CF) is generally consistent to that seen in coccolithophore bloom communities in experimental mesocosms exposed to different pCO_2 levels (Engel et al., 2005).

Of the three communities exposed to rapid changes in pH_T and Ω_C over short time periods (48 h) in this study, the response in terms of CP, cell-CF and coccolithophore cell numbers was muted in the slower growing community (Norwegian Trench) indicating either reduced sensitivity or that the experiment was too short to detect changes. Similar results were obtained in terms of phytoplankton biomass and productivity at this location in longer-term (96 h) bioassays (Richier et al., 2014). The response in CP and cell-CF to nutrient addition was rapid and clearly detectable in both the fast and slow growing coccolithophore communities of the North Sea and Norwegian Trench, but only under ambient pCO_2. The lack of response to nutrient addition by coccolithophores at elevated pCO_2 implies that the communities were unable to respond to nutrient addi-

BGD
11, 2685–2733, 2014

tion and failed to utilize nutrients to the same degree as under ambient pCO_2. Similar conclusions were drawn from trends in total phytoplankton biomass and production in the long-term pCO_2 bioassay experiments (Richier et al., 2014) which ran in parallel to the experiments presented here.

Generally, the response of the coccolithophore communities sampled in shelf waters in June 2011 to changing carbonate chemistry was variable, with negative responses to decreasing pH in two of the short-term experiments and no response in a third. Little to no response was seen along the natural gradient in pH_T and Ω_C sampled during the cruise, which may either mean that the gradients were not strong enough to detect a response or (more likely) that the communities sampled were perfectly adapted to variations of in situ carbonate chemistry. Recent analysis of long-term observations of coccolithophores in the North Sea has shown an increase in coccolithophore occurrence over the last few decades, despite a trend of decreasing pH (Beare et al., 2013). Our study also highlights these variable responses to carbonate chemistry in NW European shelf waters, which are undoubtedly complex, appear mediated by changes in growth rates and/or cellular calcification, and are inter-linked with the other growth limiting factors (irradiance, nutrients).

5 Conclusions

During June 2011 coccolithophores formed only a small (< 5 %) contribution to total primary production in waters around the NW European shelf, despite the dominance of community biomass and primary production by nano-flagellates. This small contribution to overall community activity was evident in a wide range of coccolithophore communities, including those in bloom conditions, with high detached coccolith concentrations and high CP rates (E1, North Sea), as well as those in a diatom bloom, with high CP rates and cell numbers (Helgoland), and those in a nano-flagellate bloom where total PP was > 220 mmol C m^{-2} d^{-1} (PEACE site). Despite these small contributions to pelagic production, the CP rates measured in shelf waters were of the same

BGD
11, 2685–2733, 2014

magnitude as those measured in similar studies in shelf waters and oceanic coccolithophore blooms (see Poulton et al., 2007, 2013). The cruise average integrated CP (2.6 mmol C m^{-2} d^{-1}) is equivalent to 0.26 g $CaCO_3$ m^{-2} d^{-1} (molecular weight of $CaCO_3$ taken as 100), which is only slightly lower than the 0.36 g $CaCO_3$ m^{-2} d^{-1} average for measurements taken during late summer in the Iceland Basin (Poulton et al., 2010) but ~ 100–1000 times lower than estimates of calcification rates by benthic invertebrates such as echinoderms and molluscs in shelf waters (e.g. Lebrato et al., 2010).

Variability in CP by the bulk community around the northwest European shelf was mediated by changes in coccolithophore cell numbers, species composition and cell-CF in both in situ conditions and in experimental bioassays where the response to nutrient addition and pCO_2 changes were examined. Significant coccolithophore responses to nitrate and phosphate addition as well as sensitivity to rapid decreases in pH_T (~ 0.3 units) and a rough halving of Ω_C were also observed in two of the three bioassays, with the North Sea community responding to both sets of treatments (Fig. 7). Although the sensitivity to pCO_2 manipulation appeared most muted in the bioassay with the slowest (net) growth rates (< 0.5 d^{-1}), the coccolithophore response to nutrient addition was seen in communities exhibiting both high and low growth rates. The coccolithophore response to rapid changes in pH_T and Ω_C involved either decreases in growth rates and/or cell-CF, which when combined together led to decreased community CP. As in the longer term (96 h) experiments (Richier et al., 2014), elevated pCO_2 resulted in a decrease in nutrient utilization by the coccolithophore communities. Taken together these results highlight the variable response of natural coccolithophores to environmental manipulation and the challenge of examining potential ocean acidification responses without understanding and accounting for diversity in coccolithophore eco-physiology.

Acknowledgements. Financial support for A.P. came from NERC via a postdoctoral fellowship (NE/F015054/1) and from the UK Ocean Acidification research programme (NE/H017097/1). Datasets associated with this study are available from the British Oceanographic Data Cen-

BGD
11, 2685–2733, 2014

tre (www.bodc.ac.uk/projects/uk/ukoa/data_inventories/cruise/d366/). Support for co-authors also came from UKOA via NERC grants NE/H017097/1 to M.S., NE/H01718/1 to J.Y., NE/H017062/1 to D.S., NE/H017348/1 to S.R., C.D. and E.A., and NE/H017038/1 to D.C.E.B. and G.L. We would also like to thank the officers and crew of the RRS *Discovery*, the technical staff from the National Marine Facilities, and Toby Tyrrell as lead PI for the "Sea-surface consortium". Further thanks go to Stephanie Henson (NOC), Rob Thomas (BODC) and Mariana Ribas-Ribas (University of Southampton) for help with access to MODIS satellite images and cruise data. MODIS Aqua satellite data was obtained from the NASA Ocean Colour distributed archive (http://oceancolor.gsfc.nasa.gov/).

References

Bakker, D. E. and Lee, G. A.: In situ observations of dissolved inorganic carbon, alkalinity and the partial pressure of carbon dioxide, in: Cruise Report D366/367, edited by: Richier, S. 6 June–10 July 2011, UK Ocean Acidification Research Program, 27–31, 2012.

Bakker, D. C. E., Nielsdóttir, M. C., Morris, P. J., Venables, H. J., and Watson, A. J.: The island mass effect and biological carbon uptake for the subantarctic Crozet Archipelago, Deep-Sea Res. Pt. II 54, 2174–2190, 2007.

Balch, W. M., Kilpatrick, K. A., Holligan, P., Harbour, D., and Fernández, E.: The 1991 coccolithophore bloom in the central North Atlantic, 2. Relating optics to coccolith concentration, Limnol. Oceanogr., 41, 1684–1696, 1996.

Balch, W. M., Drapeau, D. T., and Fritz, J. J.: Monsoonal forcing of calcification in the Arabian Sea, Deep-Sea Res. Pt. II, 47, 1301–1337, 2000.

Beare, D., McQuatters-Gollop, A., van der Hammen, T., Machiels, M., Teoh, S. J., and Hall-Spencer, J. M.: Long-term trends in calcifying plankton and pH in the North Sea, PLoS ONE, 8, e61175, doi:10.1371/journal.pone.0061175, 2013.

Bibby, T. S. and Moore, C. M.: Silicate:nitrate ratios of upwelled waters control the phytoplankton community sustained by mesoscale eddies in sub-tropical North Atlantic and Pacific, Biogeosciences, 8, 657–666, doi:10.5194/bg-8-657-2011, 2011.

Broecker, W. and Clark, E.: Ratio of coccolith $CaCO_3$ to foraminifera $CaCO_3$ in late Holocene deep sea sediments, Paleoceanograhy, 24, doi:10.1029/2009PA001731, PA3205, 2009.

BGD
11, 2685–2733, 2014

Charalampopoulou, A., Poulton, A. J., Tyrrell, T., and Lucas, M. I.: Irradiance and pH affect coccolithophore community composition on a transect between the North Sea and the Arctic Ocean, Mar. Ecol.-Prog. Ser., 431, 25–43, 2011.

Dickson, A. G. and Millero, F. J.: A comparison of the equilibrium constants for the dissociation of carbonic acid in seawater media, Deep-Sea Res. Pt. I, 34, 1733–1743, 1987.

Dickson, A. G., Sabine, C. L., and Christian, J. R.: Guide to best practices for ocean CO_2 measurements, PICES Special Publication 3, IOCCP report number 8, 191 pp., 2007.

Engel, A., Zondervan, I., Aerts, K., Beaufort, L., Benthien, A., Chou, L., Delille, B., Gattuso, J- P., Harlay, J., Heemann, C., Hoffmann, L., Jacquet, S., Nejstgaard, J., Pizay, M- D., Rochelle-Newall, E., Schneider, U., Terbrueggen, A., and Riebesell, U.: Testing the direct effect of CO_2 concentration on a bloom of the coccolithophorid *Emiliania huxleyi* in mesocosm experiments, Limnol. Oceanogr., 50, 493–507, 2005.

Gattuso, J.-P., Lee, K., Rost, B., Schulz, K., and Gao, K.: Approaches and tools to manipulate the carbonate chemistry, in: Guide to Best Practices for Ocean Acidification Research and Data Reporting, edited by: Riebesell, U., Fabry, V. J., Hansson, L., and Gattuso, J.-P. , Publications Office of the European Union, Luxembourg, 2010.

Grasshoff, K., Ehrhardt, M., and Kremling, K.: Methods of Seawater Analysis, Verlag Chemie, Weinhem, 1983.

Harlay, J., Borges, A. V., Van der Zee, C., Delille, B., Godoi, R. H. M., Schiettecatte, L.-S., Roevros, N., Aerts, K., Lapernat, P- E., Rebreanu, L., Groom, S., Daro, M.-H., Van Grieken, R., and Chou, L.: Biogeochemical study of a coccolithophore bloom in the northern Bay of Biscay (NE Atlantic Ocean) in June 2004, Prog. Oceanogr., 86, 317–336, 2010.

Harlay, J., Chou, L., De Bodt, C., Van Oostende, N., Piontek, J., Suykens, K., Engel, A., Sabbe, K., Groom, S., Delille, B., and Borges, A. V.: Biogeochemistry and carbon mass balance of a coccolithophore bloom in the northern Bay of Biscay (June 2006), Deep-Sea Res. Pt. I, 58, 111–127, 2011.

Haxo, F. T.: Photosynthetic action spectrum of the coccolithophorid *Emiliania huxleyi* (Haptophceae): 19'-Hexanoyloxyfucoxanthin as antenna pigment, J. Phycol., 21, 282–287, 1985.

Head, R. N., Crawford, D. W., Egge, J. K., Harris, R. P., Kristiansen, S., Lesley, D. J., Marañón, E., Pond, D., and Purdie, D. A.: The hydrography and biology of a bloom of the coccolithophorid *Emiliania huxleyi* in the northern North Sea, J. Sea Res., 39, 255–266, 1998.

BGD
11, 2685–2733, 2014

Hickman, A. E., Moore, C. M., Sharples, J., Lucas, M. I., Tilstone, G. H., Krivtsov, V., and Holligan, P. M.: Primary production and nitrate uptake within the seasonal thermocline of a stratified shelf sea, Mar. Ecol.-Prog. Ser., 463, 39–57, 2012.

Holligan, P. M., Viollier, M., Harbour, D. S., Camus, P., and Champagne-Philippe, M.: Satellite and ship studies of coccolithophore production along a continental shelf edge, Nature, 304, 339–342, 1983.

Holligan, P. M., Fernández, E., Aiken, J., Balch, W. M., Boyd, P., Burkill, P. H., Finch, M., Groom, S. B., Malin, G., Muller, K., Trees, C., Turner, S. M., and van der Wal, P.: A biogeochemical study of the coccolithophore, *Emiliania huxleyi*, in the North Atlantic, Global Biogeochem. Cy., 7, 879–900, 1993a.

Holligan, P. M., Groom, S. B., and Harbour, D. S.: What controls the distribution of the coccolithophore, *Emiliania huxleyi*, in the North Sea?, Fish. Oceanogr., 2, 175–183, 1993b.

Iglesias-Rodríguez, M. D., Brown, C. W., Doney, S. C., Kleypas, J., Kolber, D., Kolber, Z., Hayes, P. K., and Falkowski, P. G.: Representing key phytoplankton functional groups in ocean carbon cycle models: Coccolithophorids, Global Biogeochem. Cy., 16, GB1100, doi:10.1029/2001GB001454, 2002.

Jin, P., Gao, K., and Beardall, J.: Evolutionary responses of a Coccolithophorid *Gephyrocapsa oceanica* to ocean acidification, Evolution, 67, 1869–1878, 2013.

Johnson, K. M., Sieburth, J. McN., Williams, P. J. leB., and Brandstrom, L.: Coulometric total carbon dioxide analysis for marine studies: automatization and calibration, Mar. Chem., 21, 117–133, 1987.

Knauss, J.: Chapter 2: a stratified ocean, in: Introduction to Physical Oceanography, Pearson, 1996.

Krueger-Hadfield, S. A., Balestreri, C., Schroeder, J., Highfield, A., Helaouët, P., Allum, J., Moate, R., Lohbeck, K. T., Miller, P., Riebesell, U., Reusch, T. B. H., Rickaby, R. E. M., Young, J. R., Hallegraeff, G., Brownlee, C., and Schroeder, D. C.: Genotying an *Emiliania huxleyi* (Prymnesiophyceae) bloom event in the North Sea reveals evidence of asexual reproduction, Biogeosciences Discuss., in prep., this issue, 2014.

Lawson, H.: Distribution of diatoms and microzooplankton in the surface waters of the UK Shelf seas and the controlling environmental variables, M.Sc. thesis, University of Southampton, Southampton, UK, 48 pp., 2013.

Lebrato, M., Iglesias-Rodríguez, D., Feely, R. A., Greeley, D., Jones, D. O. B., Suarez-Bosche, N., Lampitt, R. S., Cartes, J. E., Green, D. R. H., and Alker, B.: Global contribution

BGD
11, 2685–2733, 2014

of echinoderms to the marine carbon cycle: $CaCO_3$ budget and benthic compartments, Ecol. Monogr., 80, 441–467, 2010.
Lessard, E. J., Merico, A., and Tyrrell, T.: Nitrate: phosphate ratios and *Emiliania huxleyi* blooms, Limnol. Oceanogr., 50, 1020–1024, 2005.
Lohbeck, K. T., Riebesell, U., and Reusch, T. B. H.: Adaptive evolution of a key phytoplankton species to ocean acidification, Nat. Geosci., 5, 346–351, doi:10.1038/ngeo1441, 2012.
Mehrbach, C., Culberson, C. H., Hawley, J. E., and Pytkowicz, R. M.: Measurement of the apparent dissociation constants of carbonic acid in seawater at atmospheric pressure, Limnol. Oceanogr., 18, 897–907, 1973.
Moore, C. M., Mills, M. M., Achterberg, E. P., Geider, R. J., LaRoche, J., Lucas, M. I., McDonagh, E. L., Pan, X., Poulton, A. J., Rijkenberg, M. J. A., Suggett, D. J., Ussher, S. J., and Woodward, E. M. S.: Large-scale distribution of Atlantic nitrogen fixation controlled by iron availability, Nat. Geosci., 2, 867–871, 2009.
Paasche, E.: A review of the coccolithophorid *Emiliania huxleyi* (Prymnesiophyceae), with particular reference to growth, coccolith formation, and calcification-photosynthesis interactions, Phycologia, 40, 503–529, 2002.
Paasche, E. and Brutak, S.: Enhanced calcification in the coccolithophorid *Emiliania huxleyi* (Haptophyceae) under phosphorus limitation, Phycologia, 33, 324–330, 1994.
Painter, S. C., Poulton, A. J., Allen, J. T., Pidcock, R., and Balch, W. M.: The COPAS'08 expedition to the Patagonian Shelf: physical and environmental conditions during the 200 coccolithophore bloom, Cont. Shelf. Res., 30, 1907–1923, 2010.
Pierrot, D. E., Lewis, E., and Wallace, D. W.R: MS Excel Program Developed for CO_2 System Calculations, Oak Ridge National Laboratory, Carbon Dioxide Information Analysis Centre, 105, US Department of Energy, Oak Ridge, 2006.
Poulton, A. J., Adey, T. R., Balch, W. M., and Holligan, P. M.: Relating coccolithophore calcification rates to phytoplankton community dynamics: regional differences and implications for carbon export, Deep-Sea Res. Pt. II, 54, 538–557, 2007.
Poulton, A. J., Charalampopoulou, A., Young, J. R., Tarran, G. A., Lucas, M. I., and Quartly, G. D.: Coccolithophore dynamics in non-bloom conditions during late summer in the central Iceland Basin (July–August 2007), Limnol. Oceanogr., 55, 1601–1613, 2010.
Poulton, A. J., Young, J. R., Bates, N. R., and Balch, W. M.: Biometry of detached *Emiliania huxleyi* coccoliths along the Patagonian Shelf, Mar. Ecol.-Prog. Ser., 443, 1–17, 2011.

BGD
11, 2685–2733, 2014

Poulton, A. J., Painter, S. C., Young, J. R., Bates, N. R., Bowler, B., Drapeau, D., Lyczsckowski, E., and Balch, W. M.: The 2008 *Emiliania huxleyi* bloom along the Patagonian Shelf: ecology, biogeochemistry and cellular calcification, Global Biogeochem. Cy., 27, 1–11, 2013.

Raitsos, D. E., Lavender, S. J., Pradhan, Y., Tyrrell, T., Reid, P. C., and Edwards, M.: Coccolithophore bloom size variation in response to the regional environment of the subarctic North Atlantic, Limnol. Oceanogr., 51, 2122–2130, 2006.

Rees, A. P., Woodward, E. M. S., Robinson, C., Cummings, D. G., Tarran, G. A., and Joint, I.: Size-fractionated nitrogen uptake and carbon fixation during a developing coccolithophore bloom in the North Sea during June 1999, Deep-Sea Res. Pt. II, 49, 2905–2927, 2002.

Ribas-Ribas, M., Rerolle, V., Bakker, D. C. E., Kitidis, V., Lee, G. A., Brown, I., Achterberg, E. P., and Tyrrell, T: Carbonate chemistry inter-comparison in the Northwest European Sea, Biogeosciences Discuss., in prep., this issue, 2014.

Richier, S., Achterberg EP, Dumousseaud, C., Poulton, A. J., Suggett, D. J., Tyrrell, T., Zubkov, M. V., and Moore, C. M.: Carbon cycling and phytoplankton responses within highly-replicated shipboard carbonate manipulation experiments around the Northwest European continental shelf, Biogeosciences Discuss., in prep., this issue, 2014.

Simpson, J. H. and Sharples, J.: Introduction to the Physical and Biological Oceanography of Shelf Seas, Cambridge University Press, 448 pp., 2012.

Smith, H., Tyrrell, T., Charalampopoulou, C., Dumousseaud, C., Legge, O. J., Birchenough, S., Pettit, L. R., Garley, R., Hartman, S. E., Hartman, M. C., Sagoo, N., Daniels, C. J., Achterberg, E. P., and Hydes, D. J.: Predominance of heavily calcified coccolithophores at low $CaCO_3$ saturation during winter in the Bay of Biscay, P. Natl. Acad. Sci USA., 109, 8845–8849, 2012.

The Royal Society: Ocean Acidification due to increasing atmospheric carbon dioxide, Policy Document 12/05, The Royal Society, London, 2005.

Tyrrell, T. and Merico, A.: *Emiliania huxleyi*: bloom observations and the conditions that induce them, in: Coccolithophores From Molecular Processes to Global Impact, edited by: Thierstein, H. R. and Young, J. R., Springer-Verlag, Heidelberg, 75–90, 2004.

van der Wal, P., Kempers, R. S., and Veldhuis, M. J. W.: Production and downward flux of organic matter and calcite in a North Sea bloom of the coccolithophore *Emiliania huxleyi*, Mar. Ecol.-Prog. Ser., 126, 247–265, 1995.

BGD
11, 2685–2733, 2014

Widdicombe, C. E., Eloire, D., Harbour, D., Harris, R. P., and Somerfield, P. J.: Long-term phytoplankton community dynamics in the Western English Channel, J. Plankton Res., 32, 643–655, 2010.

Young, J. R. and Ziveri, P.: Calculation of coccolith volume and its use in calibration of carbonate flux estimates, Deep-Sea Res. Pt. II, 47, 4679–1700, 2000.

Young, J. R., Poulton, A. J., and Tyrrell, T.: Morphology of *Emiliania huxleyi* coccoliths on the North West European Shelf – is there an influence of carbonate chemistry?, Biogeosciences Discuss., accepted, 2014.

BGD

11, 2685–2733, 2014

Table 1. Hydrographic characteristics of productivity stations sampled in north-west European shelf waters. Including station names, date sampled, station position, CTD number, mixed layer depth (ML-D), mixed layer temperature (ML-T), maximum Brunt-Väisälä Frequency (N^2 max), euphotic zone depth (Z_{eup}), incidental irradiance ($Ed_{[0+]}$), average mixed layer irradiance ($\bar{E}d_{[ML]}$), nitrate+nitrite (NO_x), phosphate (PO_4), silicic acid (dSi), excess NO_x relative to phosphate (N^*), excess dSi to NO_x (Si^*), pH_T and calcite saturation state (Ω_C).

Sampling sites	Date	Latitude, Longitude	CTD	ML-D (m)	ML-T (°C)	N^2 max ($x10^3$ m^{-1})	Z_{eup} (m)	$Ed_{[0+]}$ (mol photons m^{-2} d^{-1})	$\bar{E}d_{[ML]}$	NO_x (µmol kg^{-1})	PO_4	dSi	N^*	Si^*	pH_T	Ω_C
Mingulay Reef (MRf)	8 Jun	56.47° N, 07.24° W	C07	30	11.2	0.19	28	47.6	9.4	1.1	0.1	2.1	−0.6	1.0	8.10	3.69
Atlantic coast (Atl)	11 Jun	52.08° N, 11.42° W	C15	25	12.0	0.22	38	47.3	14.6	4.4	0.2	1.7	0.4	−2.7	8.10	3.90
Celtic Sea Deep Buoy (Cel)	13 Jun	51.36° N, 05.43° W	C19	27	13.3	0.42	33	50.9	13.4	0.1	0	0.2	0	0.2	8.12	4.19
Western English Channel (E1a)	15 Jun	50.01° N, 04.22° W	C24	23	13.8	0.41	42	47.6	17.3	0.1	0	0.4	−0.1	0.3	8.11	4.19
Bay of Biscay (BBa)	19 Jun	46.29° N, 07.12° W	C29	46	15.0	0.19	40	38.9	7.3	0.9	0.1	1.1	−0.4	0.2	8.11	4.36
Bay of Biscay (BBb)	21 Jun	46.10° N, 07.13° W	C32	51	15.3	0.26	42	48.3	8.6	1.1	0.1	0.7	−0.2	−0.4	8.10	4.33
PEACE site (PEA)	22 Jun	48.00° N, 07.11° W	C34	46	14.5	0.24	33	50.9	7.9	0.3	0	1.3	−0.1	1.0	8.11	4.31
Western English Channel (E1b)	24 Jun	50.01° N, 04.21° W	C38	16	14.0	0.41	29	40.0	15.0	1.3	0.1	1.4	−0.3	0.1	8.12	4.26
Southern North Sea (sNS)	26 Jun	52.59° N, −02.30° E	C43	Bot (37)	14.6	< 0.01	16	62.3	3.0	0.7	0.1	0.7	−1.0	0	8.04	3.60
Helgoland (Hel)	27 Jun	54.18° N, −07.18° E	C45	Bot (42)	14.3	< 0.01	19	60.6	3.3	4.3	0.1	3.4	3.4	−0.9	8.08	3.81
North Sea (NSa)	29 Jun	57.43° N, −04.35° E	C54	18	13.2	0.48	35	11.9	4.6	0.3	0.2	0.4	−2.9	0.1	8.12	4.05
North Sea (NSb)	2 Jul	56.30° N, −03.36° E	C65	22	13.8	0.70	42	19.1	7.3	0.1	0.1	0.2	−0.7	0.1	8.06	3.76
Shetlands (Sh)	3 Jul	59.51° N, −04.07° E	C67	16	13.3	3.53	24	23.1	7.1	1.5	0.1	0.6	0.6	−0.9	8.11	3.65
Faroe Islands (sFI)	5 Jul	60.00° N, 05.59° W	C71	25	11.7	0.16	41	16.7	5.6	6.2	0.4	2.1	−0.6	−4.1	8.13	4.04

BGD
11, 2685–2733, 2014

Table 2. Euphotic zone integrals of total chlorophyll (Chl_{tot}), total primary production (PP_{tot}), calcite production (CP), ratio of calcite production to primary production (CP : PP), nanoplankton contributions to Chl_{tot} and PP_{tot} and coccolithophore contributions to PP_{tot} and PP_{nano}.

Sampling site	CTD	Chl_{tot} ($mg\,m^{-2}$)	PP_{tot} ($mmol\,C\,m^{-2}\,d^{-1}$)	CP	CP : PP_{tot} (mol : mol)	Nanoplankton contributions (%)		Coccolithophore contributions (%)	
						Chl_{tot}	PP_{tot}	PP_{tot}	PP_{nano}
MRf	C07	93.1	151.6	2.7	0.02	97	96	1	1
Atl	C15	40.7	127.9	4.0	0.03	91	95	2	2
Cel	C19	28.5	128.6	0.7	0.01	ND	77	< 1	< 1
E1a	C24	22.7	68.0	6.3	0.09	67	61	6	11
BBa	C29	26.2	88.1	0.6	0.01	82	87	< 1	1
BBb	C32	29.1	122.8	1.5	0.01	64	85	1	1
PEA	C34	64.5	229.9	1.2	0.01	92	93	< 1	< 1
E1b	C38	30.7	95.2	3.7	0.04	45	71	3	4
sNS	C43	29.7	89.5	0.6	0.01	85	93	< 1	1
Hel	C45	85.0	197.9	9.6	0.05	8	14	3	23
NSa	C54	25.8	52.5	1.8	0.03	90	83	2	3
NSb	C65	20.9	45.2	1.2	0.03	78	92	2	2
Sh	C67	44.4	73.5	2.1	0.03	82	88	2	2
sFl	C71	39.3	104.2	0.7	0.01	89	80	< 1	1

ND is not determined.

BGD
11, 2685–2733, 2014

Table 3. Upper euphotic zone averages (±standard deviations) of coccolithophore cellular abundances, *E. huxleyi* relative abundance, calcite production (CP), cell-normalised calcification rate (cell-CF), *E. huxleyi* coccolith distal shield lengths (DSL) and estimates of coccolith calcite content (after Young and Ziveri, 2000), and cellular coccolith production rates.

Station	CTD	Coccolithophore abundance (cells mL^{-1})	Relative *E. huxleyi* abundance (%)	CP (mmol C m^{-3} d^{-1})	Cell-CF (pmol C cell^{-1} d^{-1})	DSL (μm)	Coccolith calcite (pmol C coccolith^{-1})	Coccolith production (h^{-1})
MRf	C07	225 (46)	100 (0)	120 (22)	0.5 (0.1)	ND	ND	ND
Atl	C15	629 (18)	99.6 (0.4)	131 (35)	0.2 (0.1)	3.08 (0.39)	0.016	0.8
Cel	C19	1 (0) [26][a]	0 (0)	39 (12)	39 (12) [1.5][a]	3.36 (0.35)	0.020	119.0 [4.4][a]
E1a	C24	630 (69)	100 (–)	312 (13)	0.5 (0.01)	3.49 (0.41)	0.023	1.4
BBa	C29	35 (12)	75.6 (5.4)	18 (6)	0.6 (0.3)	2.84 (0.35)	0.012	3.0
BBb	C32	26 (3)	74.6 (9.6)	38 (5)	1.5 (0.3)	2.79 (0.18)	0.012	8.0
PEA	C34	114 (18)	60 (15.6)	46 (4)	0.4 (0.1)	3.09 (0.32)	0.016	1.6
E1b	C38	671 (31)	100 (0)	197 (25)	0.3 (0.01)	3.48 (0.35)	0.023	0.8
sNS	C43	41 (13)	99.7 (0.1)	43 (20)	1.0 (0.2)	3.47 (0.29)	0.023	2.8
Hel	C45	818 (88)	100 (–)	665 (139)	0.8 (0.1)	3.41 (0.42)	0.021	2.3
NSa	C54	376 (173)	100 (–)	54 (17)	0.2 (0.1)	3.46 (0.26)	0.022	0.6
NSb	C65	231 (0)	100 (–)	39 (11)	0.2 (0.01)	3.19 (0.36)	0.017	0.7
Sh	C67	499 (185)	99.4 (4.2)	60 (20)	0.1 (0.1)	3.18 (0.31)	0.017	0.4
sFl	C71	90 (20)	99.5 (10.7)	20 (13)	0.2 (0.2)	2.94 (0.32)	0.014	0.9

[a] Values in brackets are based on SEM counts (Poulton, unpublished).
ND is not determined.

BGD
11, 2685–2733, 2014

Table 4. Average (±standard deviation) values for variables in the short-term (48 h) bioassay experiments. Experimental treatments are: +N is 2 µm nitrate and silicate, +P is 0.2 µm phosphate and 2 µm silicate, +NP is 2 µm nitrate and silicate and 0.2 µm phosphate.

Bioassay	Treatment	pCO_2 (µatm)	pH_T	Ω_C	NO_x (µmol kg^{-1})	PO_4	dSi	Total Chl (mg m^{-3})
Bay of Biscay (2B)	Initial	340.3	8.1	4.4	0.9 (0.1)	0.1 (0.0)	1.2 (0.0)	0.6 (0.1)
	Ambient, Control	330.0 (3.7)	8.1 (0.0)	4.5 (0.0)	0.2 (0.0)	0.0 (0.0)	1.2 (0.1)	1.4 (0.0)
	Ambient, + N	340.8 (7.7)	8.1 (0.0)	4.3 (0.1)	2.3 (0.1)	0.0 (0.0)	3.2 (0.1)	1.5 (0.3)
	Ambient, +P	333.0 (2.2)	8.1 (0.0)	4.4 (0.0)	0.2 (0.1)	0.2 (0.0)	3.2 (0.0)	1.4 (0.1)
	Ambient, +NP	341.7 (5.5)	8.1 (0.0)	4.3 (0.1)	2.3 (0.1)	0.3 (0.0)	3.2 (0.0)	1.3 (0.1)
	750, Control	660.6 (6.5)	7.9 (0.0)	2.7 (0.0)	0.8 (0.0)	0.1 (0.0)	1.2 (0.0)	0.4 (0.0)
	750, +N	686.0 (12.4)	7.8 (0.0)	2.6 (0.0)	2.8 (0.1)	0.1 (0.0)	3.2 (0.1)	0.5 (0.1)
	750, +P	690.5 (6.2)	7.8 (0.0)	2.6 (0.0)	0.8 (0.0)	0.3 (0.0)	3.2 (0.0)	0.4 (0.1)
	750, +NP	685.5 (15.0)	7.8 (0.0)	2.6 (0.1)	3.0 (0.0)	0.3 (0.0)	3.2 (0.0)	0.5 (0.0)
Northern North Sea (4B)	Initial	327.3	8.1	4.0	0.3 (0.0)	0.0 (0.0)	0.3 (0.0)	0.5 (0.0)
	Ambient, Control	328.2 (7.8)	8.1 (0.0)	4.0 (0.1)	0.2 (0.0)	0.0 (0.0)	2.2 (0.1)	0.9 (0.1)
	Ambient, + N	321.4 (3.5)	8.1 (0.0)	4.1 (0.0)	1.9 (0.1)	0.0 (0.0)	2.2 (0.0)	1.0 (0.1)
	Ambient, +P	325.3 (8.7)	8.1 (0.0)	4.0 (0.1)	0.2 (0.0)	0.2 (0.0)	2.2 (0.0)	0.9 (0.1)
	Ambient, +NP	322.6 (8.8)	8.1 (0.0)	4.0 (0.1)	1.3 (0.1)	0.1 (0.0)	2.3 (0.0)	1.9 (0.2)
	750, Control	703.9 (0.4)	7.8 (0.0)	2.2 (0.0)	0.3 (0.1)	0.0 (0.0)	2.2 (0.0)	0.4 (0.1)
	750, +N	698.6 (9.7)	7.8 (0.0)	2.2 (0.0)	2.3 (0.1)	0.0 (0.0)	2.3 (0.0)	0.6 (0.1)
	750, +P	701.2 (35.8)	7.8 (0.0)	2.2 (0.1)	0.3 (0.0)	0.2 (0.0)	2.2 (0.0)	0.6 (0.0)
	750, +NP	682.4 (30.9)	7.8 (0.0)	2.3 (0.1)	2.3 (0.0)	0.2 (0.0)	2.3 (0.0)	0.7 (0.0)
Norwegian Trench (5B)	Initial	310.7	8.1	3.9	0.3 (0.0)	0.0 (0.0)	0.0 (0.0)	0.8 (0.0)
	Ambient, Control	324.0(8.0)	8.1 (0.0)	3.7 (0.1)	0.3 (0.0)	0.0 (0.0)	1.8 (0.0)	0.6 (0.0)
	Ambient, + N	312.3 (8.8)	8.1 (0.0)	3.8 (0.1)	1.7 (0.0)	0.0 (0.0)	1.7 (0.0)	1.0 (0.0)
	Ambient, +P	340.7 (8.2)	8.1 (0.0)	3.6 (0.1)	0.3 (0.0)	0.1 (0.0)	1.8 (0.0)	0.6 (0.1)
	Ambient, +NP	316.3 (10.4)	8.1 (0.0)	3.8 (0.1)	0.9 (0.1)	0.1 (0.0)	1.7 (0.0)	1.7 (0.1)
	750, Control	671.0 (34.5)	7.8 (0.0)	2.1 (0.1)	0.3 (0.0)	0.0 (0.0)	1.8 (0.0)	0.4 (0.1)
	750, +N	665.9 (17.4)	7.8 (0.0)	2.1 (0.0)	1.9 (0.1)	0.0 (0.0)	1.8 (0.0)	0.7 (0.1)
	750, +P	674.8 (20.3)	7.8 (0.0)	2.1 (0.1)	0.3 (0.0)	0.1 (0.0)	1.9 (0.0)	0.4 (0.0)
	750, +NP	692.9 (19.4)	7.8 (0.0)	2.1 (0.1)	1.5 (0.2)	0.1 (0.0)	1.7 (0.1)	1.1 (0.1)

BGD
11, 2685–2733, 2014

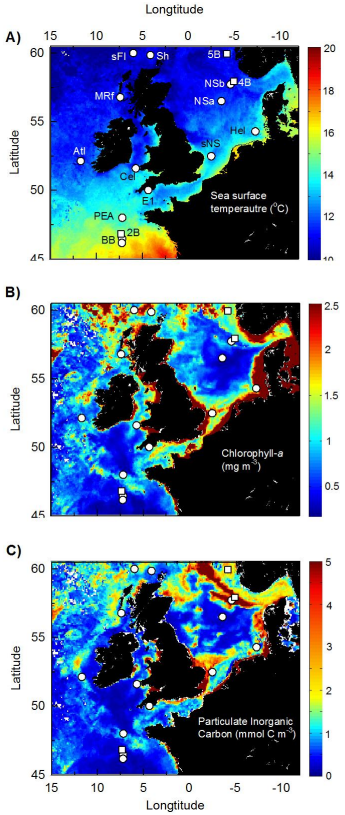

Fig. 1. Maps showing the position of the daily productivity sampling stations (circles) and short-term (48 h) experiments (squares), superimposed on MODIS composites (June 2011) of **(A)** sea surface temperature (°C), **(B)** surface chlorophyll *a*, (mg m^{-3}), and **(C)** surface Particulate Inorganic Carbon (mmol C m^{-3}).

BGD
11, 2685–2733, 2014

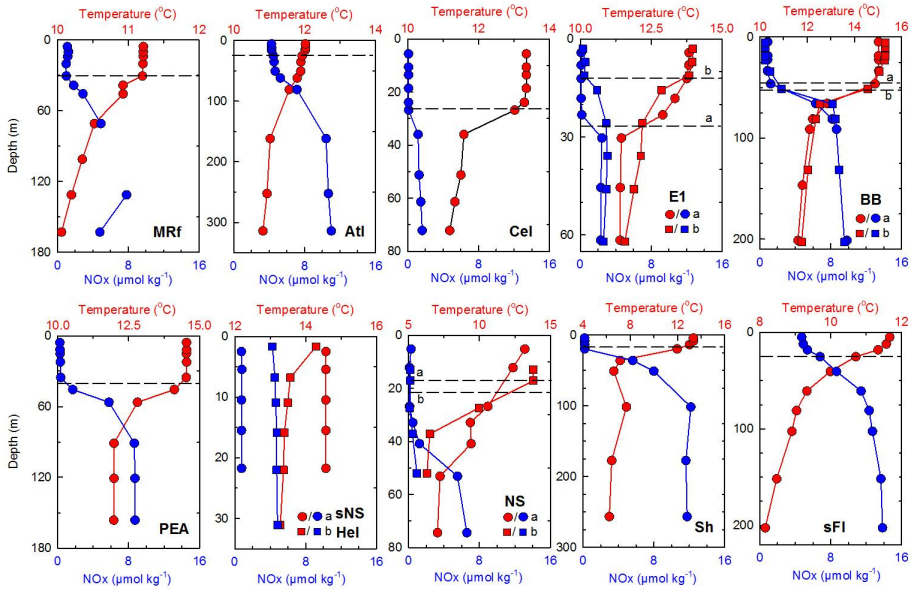

Fig. 2. Vertical profiles of temperature (°C) and nitrate+nitrite (NO_x, µmol N kg^{-1}) over the upper water column. Dashed lines indicate mixed layer depths.

BGD
11, 2685–2733, 2014

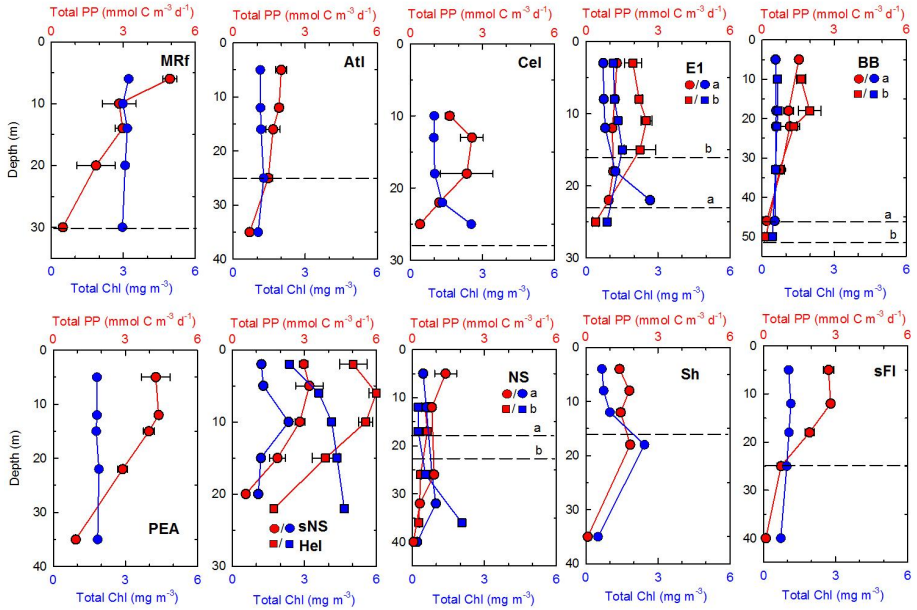

Fig. 3. Vertical profiles of total primary productivity (total PP, mmol C m^{-3} d^{-1}) and total chlorophyll (total Chl, mg m^{-3}) over the euphotic zone. Dashed lines indicate mixed layer depths.

BGD
11, 2685–2733, 2014

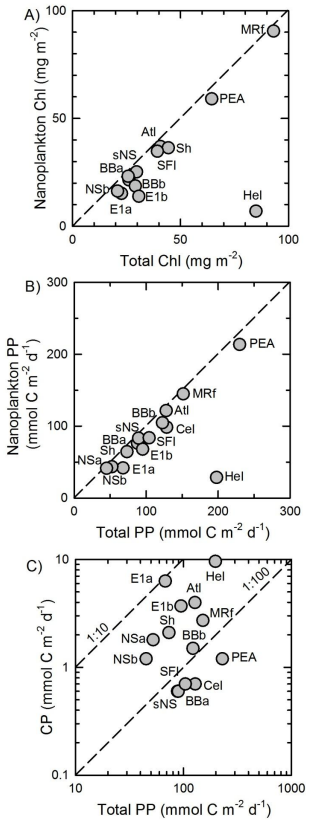

Fig. 4. Scatter plots of integrated **(A)** total Chl and nanoplankton (< 10 µm) Chl (mg m^{-2}), **(B)** total PP and nanoplankton (< 10 µm) PP (mmol C m^{-2} d^{-1}), and **(C)** calcite production (CP) and total PP (mmol C m^{-2} d^{-1}). Dashed lines in **(A)** and **(B)** indicate the 1 : 1 line while dashed lines in **(C)** indicate ratios of 1 : 10 and 1 : 100.

BGD
11, 2685–2733, 2014

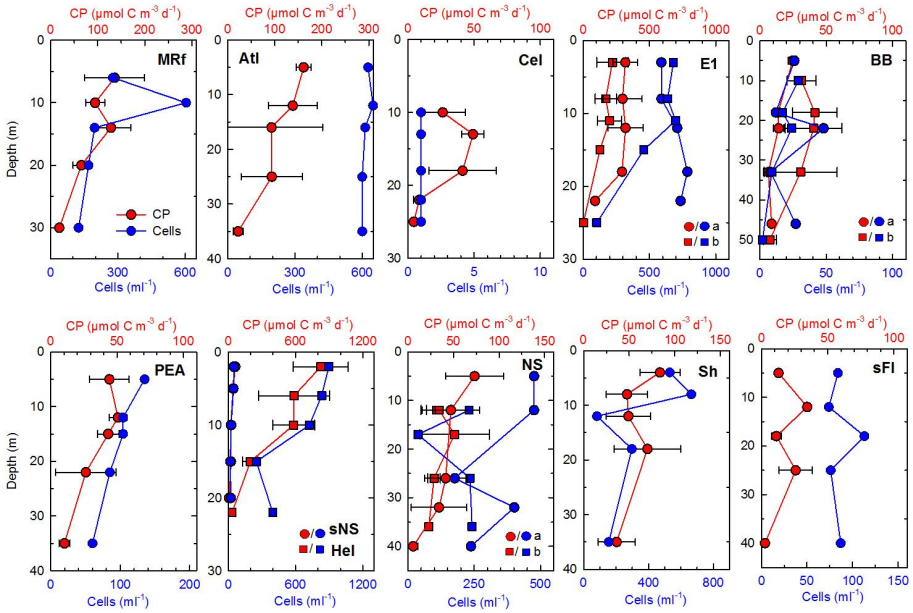

Fig. 5. Vertical profiles of calcite production (CP, µmol C m^{-3} d^{-1}) and coccosphere abundance (Cells, mL^{-1}) over the euphotic zone.

BGD
11, 2685–2733, 2014

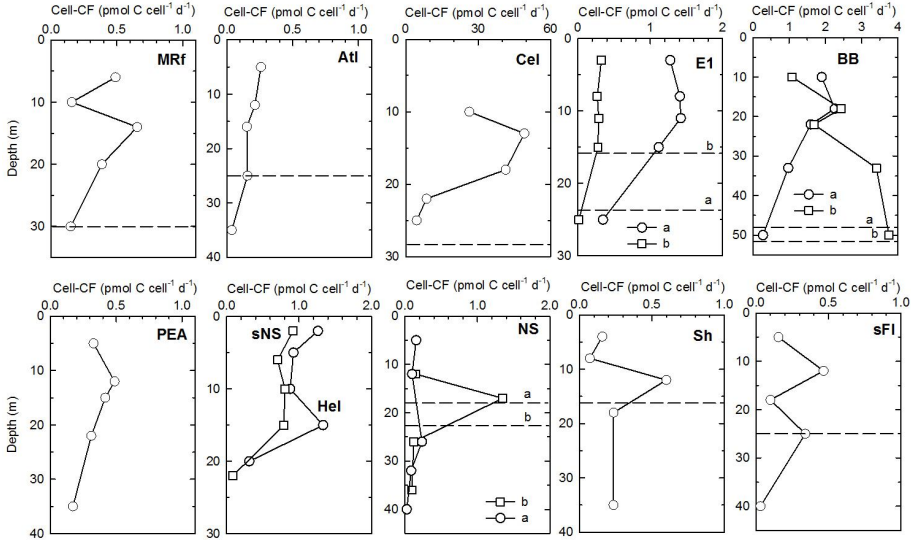

Fig. 6. Vertical profiles of cell-normalised calcite production (cell-CF, pmol C cell^{-1} d^{-1}) over the euphotic zone. Dashed line indicates mixed layer depth (MLD).

BGD
11, 2685–2733, 2014

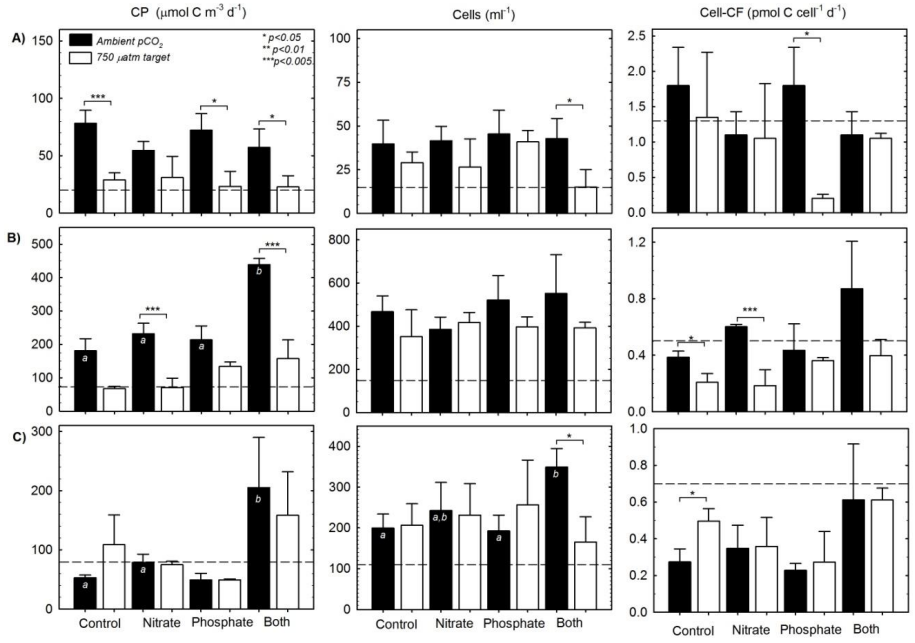

Fig. 7. Results from nutrient/pCO_2 amendment experiments for calcite production (CP), coccosphere abundance (Cells) and cell-normalised calcification (cell-CF). Experiments are from **(A)** Bay of Biscay, **(B)** Northern North Sea, and **(C)** Norwegian Trench. Dashed lines indicated average initial rates and standing stocks. Asterisks indicate significant results from pair-wise *t* tests between ambient and target 750 µatm treatments: * $p < 0.05$, ** $p < 0.01$, *** $p < 0.005$. Letters indicate significant ($p < 0.05$) groupings from one-way ANOVA and pair-wise *t* tests between nutrient treatments and controls.

BGD
11, 2685–2733, 2014